INTERNATIONAL ATOMIC ENERGY AGENCY
UNITED NATIONS EDUCATIONAL, SCIENTIFIC AND CULTURAL ORGANIZATION
INTERNATIONAL CENTRE FOR THEORETICAL PHYSICS
I.C.T.P., P.O. BOX 586, 34100 TRIESTE, ITALY, CABLE: CENTRATOM TRIESTE

UNITED NATIONS INDUSTRIAL DEVELOPMENT ORGANIZATION

INTERNATIONAL CENTRE FOR SCIENCE AND HIGH TECHNOLOGY
c/o INTERNATIONAL CENTRE FOR THEORETICAL PHYSICS 34100 TRIESTE (ITALY) VIA GRIGNANO, 9 (ADRIATICO PALACE) P.O. BOX 586 TELEPHONE 040-224572 TELEFAX 040-224575 TELEX 460449 APH I

SMR/548-4

Course on Oceanography of Semi-Enclosed Seas
15 April - 3 May 1991

"Gulf of California - General Circulation"

M. HENDERSHOTT
Scripps Institute of Oceanography
University of California - San Diego
USA

GULF OF CALIFORNIA GENERAL CIRCULATION - M. HENDERSHOTT
Trieste, 1991

Gulf Entrance.

Conditions at the entrance of the gulf are of interest because they tell us about exchange with the surrounding Pacific, both by seeing what waters at the entrance are of Pacific origin and what of gulf origin, and by the pattern of geostrophic flow in/out of the gulf. **Fig. 1** (Roden, 1972; Fig. 3) is a section from the tip of Baja California to Mazatlan. On it are visible (bottom up)

Pacific deep water; below 1000 m, S increases to about 34.7 ppm at 1500m
Pacific intermediate water; 500-1000m, S minimum 34.5 ppm and
O_2 minimum 0.1-0.2 ml/l between 600-900m
Subtropical subsurface water; 125-400m, S maximum about 34.6 ppm, water from east subtropical Pacific
California Current water; 75-125m, S minimum 33.6-34.0 pp, relatively cool (15-18°C)
Gulf water; surface-75m, S very high (34.8-35.2 ppm)

Fig. 2 (Roden 1972, Fig. 4) shows geostrophic velocity across the section relative to 1500 db.

Note (a) California Current water is concentrated on east side of section, Gulf water on west.
(b) Geostrophic outflow very strongly concentrated on west; sense of circulation viewed from above gulf is thus counterclockwise (cyclonic).
(c) Outflowing salty water is at surface, not (as in Gibraltar) at depth.
(d) These geostrophic flows are not constrained to conserve mass; inflow is 10 Sv and outflow is 12 Sv, discrepancy far too large to be precipitation, must be reference level choice, even so westward intensification of outflow probably survives correct choice.
(e) The deep O_2 minimum persists into the Gulf; bottom conditions in eastern Guaymas basin are anoxic where it touches bottom, sediments are undisturbed and individual years can be recognized in layering (Baumgartner et al, 1985).

Guaymas-Santa Rosalia Line.

Fig. 3 (Roden, 1964, Fig. 10a) shows T, S and O_2 just south of the Guaymas-Santa Rosalia line.

Below about 300 m the water is clearly of Pacific origin; the intermediate water salinity minimum at 800-1000 m is only slightly diluted relative to its value at the entrance (34.5->34.55 ppm), the associated oxygen minimum extends from 400 - 1000 m.

Above 300 m structure is variable. Sometimes (**Fig.4b**; Roden, 1964, Fig.11b) high salinities are found to the west and low salinities to the east, as the entrance counterclockwise (cyclonic) circulation pattern would suggest, but this is by no means always the case (**Fig. 4a,c**; Roden, 1964, Fig.11a.c).

Bray (1988a) has worked up geostrophic flow across the Guaymas-Santa Rosalia line for all the months for which data were available up to 1986. **Fig. 5** (composite of Bray, 1988a, Figs. 6 8 for line 50) shows this flow relative to the density surface σ_θ=26.8 at roughly 400 m. Circulation is counterclockwise (cyclonic) in summer (June, August) as well as in late winter (March) and spring (April). But in May and October flow along Baja California appears to be northward, and the pattern in November is not simple. No simple seasonal pattern for the circulation thus emerges.

Yet there is clear evidence of seasonal upwelling. Vertical profiles of temperature averaged over November 1984 and May-July 1984 at Guaymas and Santa Rosalia are shown in **Fig 6** (Merrifield and Winant, 1989, Fig. 8). They show coldest surface water and the lowest vertical gradients in winter at Guaymas (when winds generally blow down gulf) and in summer at Santa Rosalia (when winds generally blow up gulf). An upelling episode has been documented by Badan et al (1985) in IR satellite images taken in late March and april of 1980. **Fig. 7** (Composite of Fig. 2 and Fig.4 of Badan-Dangon et al, 1985) shows cold water appearing along the eastern edge of the Gulf from Tiburon almost to Topolobampo over a period of about a week, apparently in response to a burst of down gulf winds. The cold plume stretching westwards from about the location of Guaymas is frequently observed in satellite images of the Gulf. I know of no direct observations of the depth to which it extends. It might be partly responsible for the complexity of salinity and geostrophic circulation along the Guaymas-Santa Rosalia line evident in Figs. 4 and 5.

Given the suggestion that seasonal upwelling occurs, and given particularly the event documented by Badan-Dangon et al (1985), it is remarkable that measured currents offshore of Guaymas *do not respond strongly* to fluctuations of the wind field over the Gulf. **Fig. 8** shows stick plots of currents measured across the Guaymas-Santa Rosalia line at moorings maintained from May to October of 1984 (Merrifield and Winant, 1989, Fig. 19), and **Fig. 9** shows the alongshore component of velocity at Guaymas, Santa Rosalia and the midpoint of the line between them together with the wind stress (Merrifield and Winant, 1989, Fig. 20). *There is little correlation between wind events and current events.*. This is in marked constrast with the situation in upwelling regions such as the California coast, where there is very significant correlation between alongshore currents and alongshore winds. Table 1 summarizes such correlations for a number of regions, including the Gulf of California (Merrifield and Winant, 1989, Table 6). Merrifield and Winant suggest that the reason for this is along the California coast stratification is weaker and winds are stronger than in the Gulf. The appreciable variability over time scales of days to weeks that does appear is generated outside the Gulf and propagates into the Gulf in coastally trapped continental shelf waves (Merrifield and Winant, 1989); this part of the variability will be examined in a later lecture.

The longest records of the 1983-1984 deployment of current meters along the Guaymas-Santa Rosalia line provide a little more information about the seasonal pattern of circulation. At mid basin the 50 m flow shifts from up gulf to down gulf in September 1984, at the same time the wind stress shifts to down gulf and the 10 m flow at Santa Rosalia shifts from down gulf to up gulf (**Fig. 10**; composite of: wind stress Merrifield and Winant, 1989, Fig. 19; M11 10 m current at Santa Rosalia May-Nov 83, M9 50m midbasin currents May-Nov 84 from Merrifield et al, 1987). This shift does not penetrate up over the shelf to Guaymas (**Fig 11**; Winant and Merrifield, 1989, Fig. 17). Bray's May 1984 geostrophic flow across the Guaymas Santa Rosalia line (Fig. 5) shows up gulf flow at Santa Rosalia and down gulf flow in mid basin; it thus appears to reflect the situation just before flow at Santa Rosalia shifts to down gulf flow in May-June of 1984 (Fig. 11).

On interannual scales the circulation in the upper waters of the Gulf appears to be strongly influenced by El Nino events. The seasonal cycle (excluding El Nino years) of water properties along the Guaymas-Santa Rosalia line is summarized in the TS plots of **Fig. 12a** (Robles and Marinone, 1987, Fig.3). The lowest salinities (34.8-35.0 ppm) occur on the σ_θ=24.5-25.0 surfaces (upper hundred meters in late summer and near the surface at other times). There is a seasonal salinity minimum from June through August, evidently of California Current water origin. But similarly low salinities appear on these surfaces in March and October of 1983 (**Fig. 12b,c**; Robles and Marinone, 1987, Fig. 2b,g). Robles and Marinone argue from high salinities observed very near the coast at Guaymas in 1983 that these low salinities are *not* the result of anomalously high precipitation but rather are associated with the strong El Nino of 1982-3 (based on indices of Quinn et al, 1978).

The anomalous water is however not simply California current water because it is anomalously warm as well as anomalously fresh. It is evident from **Fig. 13** (Robles and Marinone, 1987, Figs. 7 and 5) that monthly mean sea level at Guaymas is anomalously high during El Nino years. The positive anomaly of sea level during El Nino had previously been documented in Gulf-wide average by Baumgartner and Christensen (1985), who found that gulf-averaged sea level anomaliies respond only to Pacific-wide indices of El Nino but not to Pacific-wide indices of north Pacific gyre variability (**Fig. 14a,b**; composite of Fig. 2, Fig. 3, Fig. 9, EOF's Figs 5,6,7, Table 2, all from Baumgartner and Christensen, 1985). The anomalouswater that was carried into the Gulf during the 1982-3 El Nino must thus have been a mixture of fresh California Current water and Warm Subtropical Subsurface water; how this happens in El Nino years is not well understood.

Exchange Between the Northern Gulf and Guaymas Basin.

Because the northern Gulf is broad and exposed to dry winds from the deserts to the north and east, it is natural to suppose that evaporation is great there and that, consequently, the northern Gulf should be a source of saline water. It is tempting but incorrect to further suppose that the exchange between the northern Gulf and Guaymas basin across the intervening shallow sills is in the same sense as the exchange between the Mediterranean and the Atlantic across Gibraltar, where salty water flows out of the evaporative basin just at sill depth. It turns out that although the northern Gulf is indeed a source of saline water because evaporation there is intense, the northern gulf is actually heated by the sun-atmosphere so that it produces saline but warm water. That water leaves the northern gulf over the sills near the surface. Consequently water at sill depth flows *from* Guaymas basin *into* the northern Gulf.

Various estimates of insolation, back radiation, latent heat flux and sensible heat flux in annual average over the northern gulf are summarized in **Table 2**. They are due to Roden and Emilson (1979), Lavin and Organista (1988), Bray (1988a), and Paden (1990). The estimate of Roden and Emilson (1979) implies that the northern gulf looses heat to the atmosphere, but this now appears to be an artifact arising from overestimation of wind speed and underestimation of relative humidity (Lavin and Organista, 1988); their estimate of evaporation in the northern Gulf was over 3 m/yr. Lavin and Organista (1988) extrapolate coastal data from 1979 to 1986 over the northern Gulf to obtain an estimated yearly evaporation of about 0.9 m/yr. Paden (1990) uses meteorological data from the network of stations maintained in 1983-1984 (Merrifield et al, 1987) to obtain a one year average evaporation of about 1.6 m/yr. Bray (1988a) estimates the heat flux across the Guaymas-Santa Rosalia line using the monthly averages (where available) of temperature, salinity and geostrophic velocity shown above in Fig. 5. If all the estimates of Roden and Emilson (1979) shown in Table 2 except the very high latent heat loss are accepted, then knowledge of the total heat flux results in a reduction of the latenet heat loss from 300 w/m^2 to about 100 w/m^2 (third column of Table 2). This corresponds to a northern Gulf yearly evaporation rate of .95 m/yr.

Bray (1988a) estimates the annual average exchange of water across the Guaymas-Santa Rosalia line to be about 0.9 Sv. In accord with the fact that the northern gulf both evaporates and is warmed, this exchange has to involve cold Pacific water flowing up gulf at depth and warm water of northern gulf origin flowing down gulf near the surface. Such a pattern is clearly visible in the average across the Guaymas-Santa Rosalia line shown in **Fig. 15** (Bray, 1988a, Fig. 17). It is clear that this meridional exchange fluctuates strongly with season, being most intense in the summer. Whether causally or coincidentally, the summer months are the time when the net heating of the northern gulf is most intense while the northern gulf actually looses heat to the atmosphere in the winter (**Fig. 16**; composite of Lavin and Organista, 1988 Fig.2 and Paden, 1990, Fig.6 of Ch. 3). When the exchange is strongest, in the summer, the outflow of saline water from the

northrn gulf occurs not right at the surface but some distance below; the northward flow of water right at the surface is presumably driven by summertime up-gulf winds.

Exchange Between Canal de Ballenas and Guaymas Basin.

Exchange between the northern gulf and Guaymas basin takes place through the narrow channels that connect Guymas basin (to the south) with Canal de Ballenas via the San Lorenzo sill, and with San Esteban Basin via the San Esteban sill. Both portions of this exchange are lumped together in the exchange across the Guaymas-Santa Rosalia line documented by Bray (1988a).

The exchange across San Lorenzo sill has been examined directly by Badan-Dangon and Hendershott (1985, 1991). Current meter measurements over San Lorenzo sill in November-December 1984 and January 1990 showed strong flow 10 meters from the bottom into Canal de Ballenas from Guaymas basin. The January, 1990, record is shown in **Fig.17** (Badan-Dangon et al, 1991, Fig. 1). The flow at 10 meters into Canal de Ballenas is most obvious at neap tides, when tidal currents are least energetic. 100 meters above the bottom the subtidal flow is from Canal de Ballenas to Guaymas Basin. An acoustic doppler logger profile of currents along a line in Guaymas basin crossing the in/out flow over San Lorenzo sill exactly at slack neap tides (**Fig.18**; Badan-Dangon et al, 1991, Fig. 2) clearly shows deep flow into Canal de Ballenas and higher outflow. The exchange in this section amounts to about 0.2 Sv.

A north-south section (**Fig. 19**; Alvarez-Borrego et al, 1978, Fig.6) of properties along the entire gulf passing over San Lorenzo sill and Canal de Ballenas into the northern gulf suggests why this Mediterranean-in-reverse exchange might persist. Water columns just north of San Lorenzo sill in Canal de Ballenas are much warmer and hence less dense as well as more vertically well mixed than water columns just south of San Lorenzo sill in Guaymas basin. This density distribution can support a horizontal pressure gradient force that is into Canal de Ballenas at sill depth but out of Canal de Ballenas higher up in the water column.

The difference in water properties between Canal de Ballenas and Guaymas basin points to strong inputs of heat, salt and oxygen either from the surface or from the far northern gulf through the northern end of Canal de Ballenas. The vertical near homogeneity of the water columns in Canal de Ballenas is probably maintained by vertical mixing associated with the very strong tidal currents that flow over San Lorenzo sill and in the narrow (5-10 km) channel itself.

Badan-Dangon et al (1985) document the continued presence of anomalously cold surface waters in the vicinity of San Lorenzo and San Esteban sills. Evidence that this is maintained by tidal mixing is given by Paden et. al. (1990), who find that the amplitude of the EOF of sea surface temperature that contains most of variance of temperature of this cold patch (**Fig. 20**; Paden, 1990, Fig. 14) is very well correlated with the spring-neap tidal cycle in the northern Gulf (**Fig. 21**; Paden et. al. , 1990, Fig. 20). The continued presence of cold water at the surface in these regions there raises the net yearly averaged air-sea heat flux to the highest values it attains in the entire gulf (**Fig. 22**; Paden, 1990, Fig. 6, Ch. 3).

A significant part of the total exchange between Guaymas Basin and the northern gulf thus appears to occur across San Lorenzo sill and through Canal de Ballenas. We do not however know how much of the exchange across San Lorenzo sill continues through the length of Canal de Ballenas to its northern end as exchange between Canal de Ballenas and the far northern gulf. Direct current meter measurements at the north end of the channel shown in Fig. 17 (Badan-Dangon et al, 1991, Fig. 1) suggest far less exchange there than occurs over San Lorenzo sill, but a comparison of these with hydrographic and doppler logger measurements has not yet been carried out.

Water Mass Formation in the Far Northern Gulf.

The far northern gulf (e.g. the northern gulf excluding Canal de Ballenas) is clearly a source of saline water in yearly average. But the processes that produce this water and get it from the regions where it is formed to places in ultimately in communication with San Lorenzo and San esteban sills are not well documented.

Evaporation over very shallow water is known to produce high salinities in the far northern Gulf. In March 1973, Villasenor (1974) found salinities greater than 36.0 ppm in the old Colorado River delta at the very tip of the northern gulf. Salinities above 35.7 ppm were found (counterclockwise) along the coast from Puerto Penasco to south of San Felipe (**Fig. 23**; Villasenor, 1974, Fig. 10).

This water probably is carried southward by the large-scale horizontal circulation of the far northern gulf, and is mixed both laterally and to depth by tidal mixing (particularly in shallower water) or vertically by localized convection.

Virtually nothing has been published about the wind driven subtidal flow of the northern gulf, although it is likely to be particularly energetic in wintertime when strong winds away from the high pressure region then commonly found over the southwestern U.S. Likewise, residual tidal circulation is probably of importance since the spring tidal range, and tidal currents, are so great in the northern gulf (Quiros, 1983). Bray (1988a) has worked up the geostrophic circulation across several lines traversing the northern gulf from west to east. The pattern is not simple, although a counterclockwise (cyclonic) component dominates the summer months (**Fig. 24**; Bray 1988a, Fig.5,6,8 for line 500). A spatial map of 10/100 dynamic height in March 1985 shows clockwise (anticyclonic) circulation roughly centered over Wagner Basin (Fig. 25; Bray 1988b, Fig. 15).

The center of this anticyclonic gyre contains water of salinity greater than 35.3 ppm (**Fig.25**); it must have come from the very shallow coastal rim of the far northern gulf (Fig.23).It does not however there extend to the bottom (**Fig. 26**; Bray 1988b, Fig. 16). Instead convection from surface to bottom appears to have occured further to the north, at the head of Wagner basin where the depth is about 160 m. Evidence for this is the presence of high salinity bottom water here but not at neighboring stations (**Fig. 27**; Bray 1988b, Fig. 9), and the great variability in vertical profiles there over about a week (**Fig. 28**; Bray 1988b, Fig. 8).

General Circulation Bibliography

Roden, G. I. (1972). Thermohaline Structure and Baroclinic Flow Across the Gulf of California Entrance and in the Revilla Gigedo Islands Region. Jour. Phys. Oceanog. 2, pp. 177-183.

Baumgartner T., V. Ferreira-Bartrina, H. Schrader and A Soutar (1985). A 20 year varve record of siliceous phytoplankton variability in the Central Gulf of California. Marine Geology, 64, pp. 113-129.

Roden, G. I. (1964). Oceanographic aspects of the Gulf of California, in Marine Geology of the Gulf of California, Mem. Assoc. Pet. Geol., 3, edited by T. J. Van Andel and G. G. Shor, pp 30-58. American Association of Petroleum Geologists, Tulsa Okla., 1964.

Bray, N. A. (1988a). Thermohaline Circulation in the Gulf of California. Jour. Geophys. Res. 93, pp. 4993-5020.

Merrifield, M. A. and C. D. Winant (1989). Shelf Circulation in the Gulf of California: A Description of the Variability. Jour. Geophys. Res. 94, pp. 18133-18160.

Badan-Dangon, A., C. J. Koblinsky, T. Baumgartner (1985). Spring and summer in the Gulf of California: observations of surface thermal patterns. Oceanologica Acta, 8, pp. 13-22.

Merrifield, M. A., C. D. Winant, J. M. Robles, R. T. Guza, N. A. Bray, J. Garcia, A. Badan-Dangon, and N. Christensen Jr. (1987). Observations of currents, temperature, pressure and sealevel in the Gulf of California 1983-1985. A data report, SIO Ref. 87-6, 192 pp., Scripps Inst. of Oceanogr., La Jolla, Calif, 1987.

Robles, J. Ma. and S. G. Marinone (1987). Seasonal and internnnual variability in the Guaymas Basin of the Gulf of California. Cont. Shelf. Res., 7, pp. 715-733.

Quinn, W. H., D. O. Zopf, K. S. Short and R. T W. Kuo Yang (1978) Historical trends and statistics of the Southern Oscillation El Nino and Indonesian droughts. Fishery Bulletin, 76, 663-678.

Baumgartner, T. and N. Christensen (1985). Coupling of the Gulf of California to large-scale interannual climatic variability. Jour. Mar. Res. 43, 825-848.

Roden, G. I. and I. Emilsson (1979). Physical Oceanography of the Gulf of California, in Simposio El Golfo de California, Edited by A. Ayala-Castanares, F. B. Phleger, R. Schwartzlose, and A. Laguarda, Universidad Nacional Autonomia de Mexico, Mexico City, 1979.

Lavin. M.F. and S. Organista (1988). Jour. Geophys. Res. 93, pp. 14033-14038.

Paden, C. A., M. R. Abbott and C. D. Winant (1990). Tidal and atmospheric forcing of the upper ocean in the Gulf of California Part I: sea surface temperature variability. Jour. Geophys. Res.

Paden, C. A. (1990). Tidal and atmospheric forcing of the upper ocean in the Gulf of California. PhD thesis, University of California in San Diego, 1990, 86 pp.

Badan-Dangon, A. and M. C. Hendershott (1985). On the flow into Ballenas Channel. IAMAP/IAPSO Joint Assembly, Honolulu: 46, 1985.

Badan-Dangon, A. , M. C. Hendershott and M. F. Lavin (1991). UNderway doppler-logger current profiles in the Gulf of California. EOS, Transactions, American Geophysical Union, in press.

Alvarrez-Borrego, AS., J. A. Rivers, G. Gaxiola Castro, M. Acosta Ruiz and R. A. Schwartzlose (1978). Nutrientes en el Golfo de California. Ciencias Marinas (Mex), 5, pp 53-71.

Quiros, G. E. (1983). Circulacion Residual en el Golfo de California. Un modelo numerico. M. Sc. Thesis CICESE, 98 pp.

Villasenor, A. C. (1974). Hidrologia de la parte norte del Golfo de California a finales de invierno. Tesis de licenciatura, Escuela Superior de Ciencias Marinas, Universidad Autonoma de Baja California, Ensenada, 53 pp., 1974

Table 1

TABLE 6. Comparison of Stratification, Wind Stress, and Wind-Current Correlations Measured During Different Field Studies

Experiment	Brunt-Vaisala Frequency N cpd	Mean Alongshelf Wind, $\langle\tau^y\rangle$, Pa	St. Dev. of Alongshelf Wind, $\tau^{y\prime}$, Pa	Correlation Between Near-surface, Midshelf Alongshelf Current and Wind (v,τ^y)
CODE-2	100	-0.12	0.12	0.7 – 0.8
NSFE79 (winter)	30	0.01	0.27	0.63
S. California (winter)	50	-	0.01	0.41 – 0.69
NSFE79 (summer)	280	0.01	0.05	0.36
Gulf of California (winter)	140–170	-0.01	0.02	0.2
Peru	100	0.06	0.01	0.18
Gulf of California (summer)	190–240	0.01	0.01	0.02
S.California (summer)	~ 250	-	0.01	-0.46

Table 1. Air-Sea Fluxes for the Northern Gulf of California (references in text)

	Roden and Emilson	Lavin and Organista	Bray	Paden
Insolation (w/m^2)	290	206	270	243
Back rad. (w/m^2)	-75	-52	-95	-53
Latent (w/m^2)	-300	-67 -82	-110 - 80	-109
Sens. (w/m^2)	-30	-4	-45	-7
Net (w/m^2)	-115	68 83	20 50	71

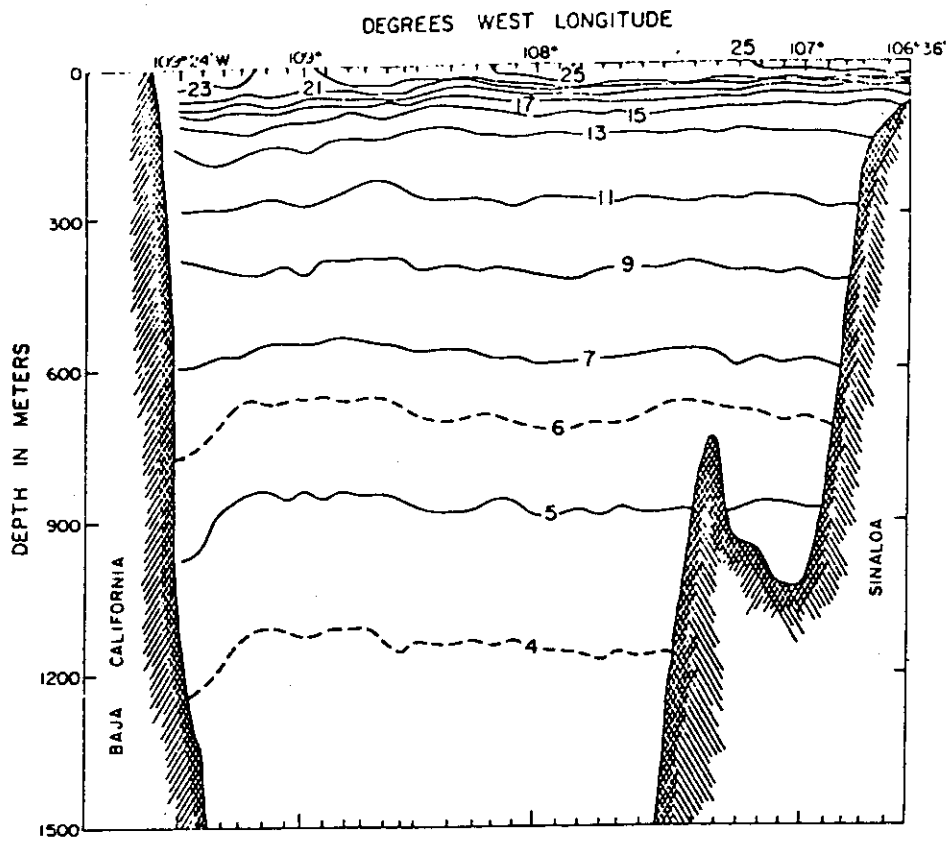
DEGREES WEST LONGITUDE
108°
25
107°
106°36'
DEPTH IN METERS
0
300
600
900
1200
1500
23
21
17
15
13
11
9
7
6
5
4
BAJA CALIFORNIA
SINALOA

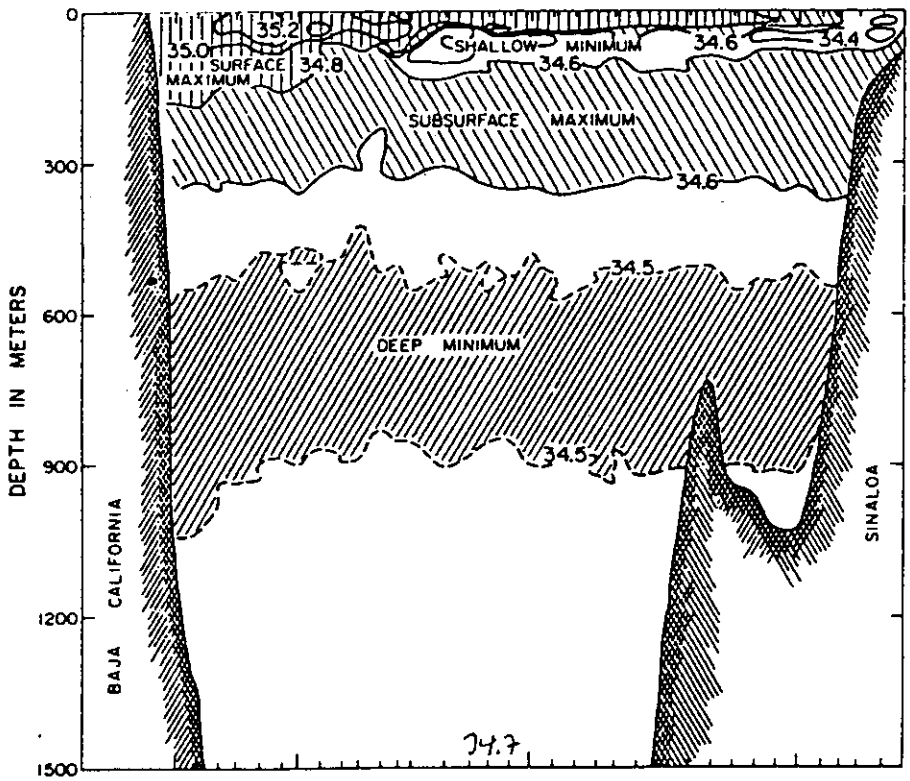
DEPTH IN METERS
0
300
600
900
1200
1500
35.2
35.0
SURFACE MAXIMUM
34.8
SHALLOW MINIMUM
34.6
34.4
SUBSURFACE MAXIMUM
34.6
34.5
DEEP MINIMUM
34.5
34.7
BAJA CALIFORNIA
SINALOA

610

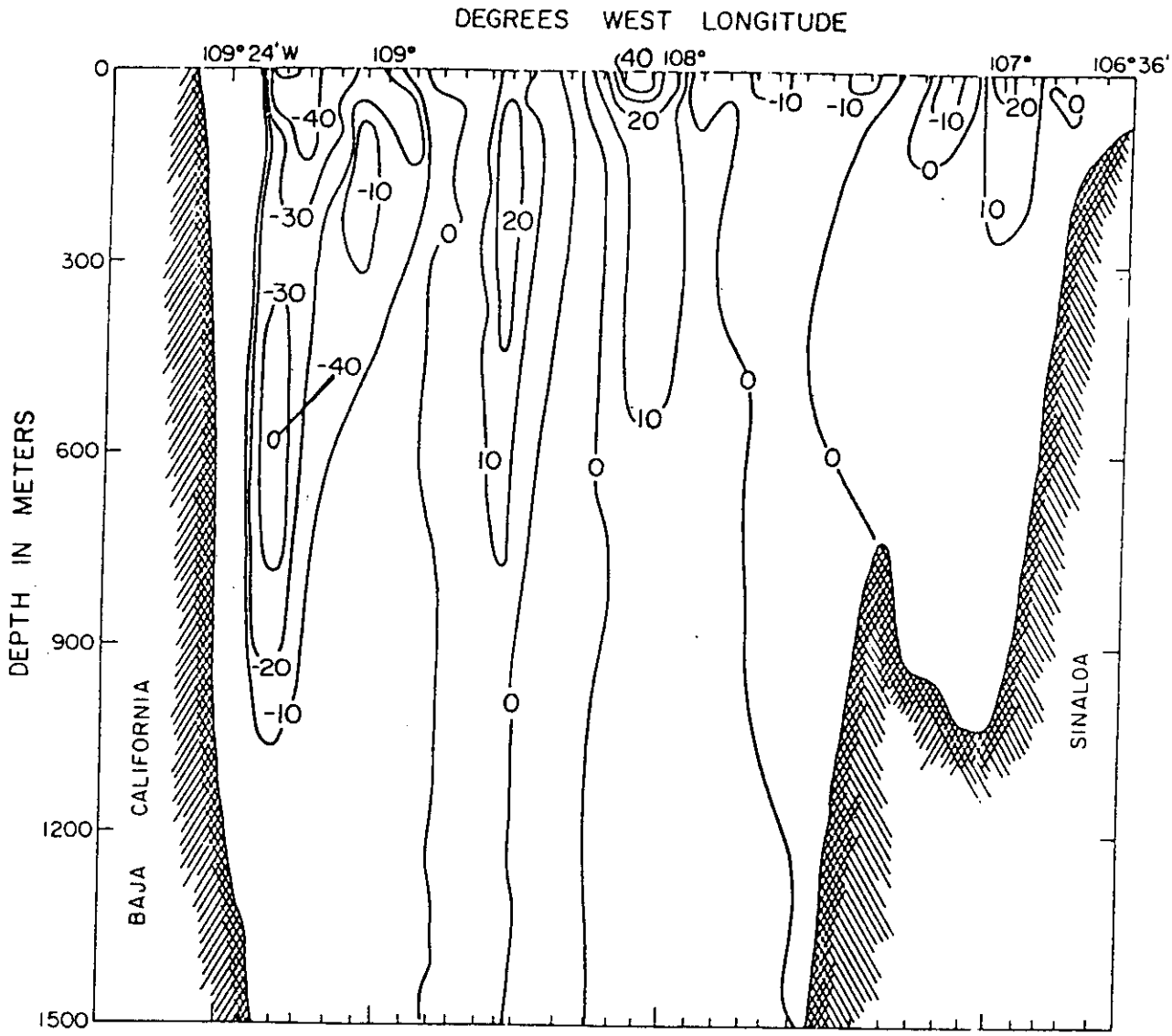
DEGREES WEST LONGITUDE
109°24'W
109°
108°
107°
106°36'
DEPTH IN METERS
0
300
600
900
1200
1500
BAJA CALIFORNIA
SINALOA
-40
-30
-20
-10
0
10
20
40

GC (2)

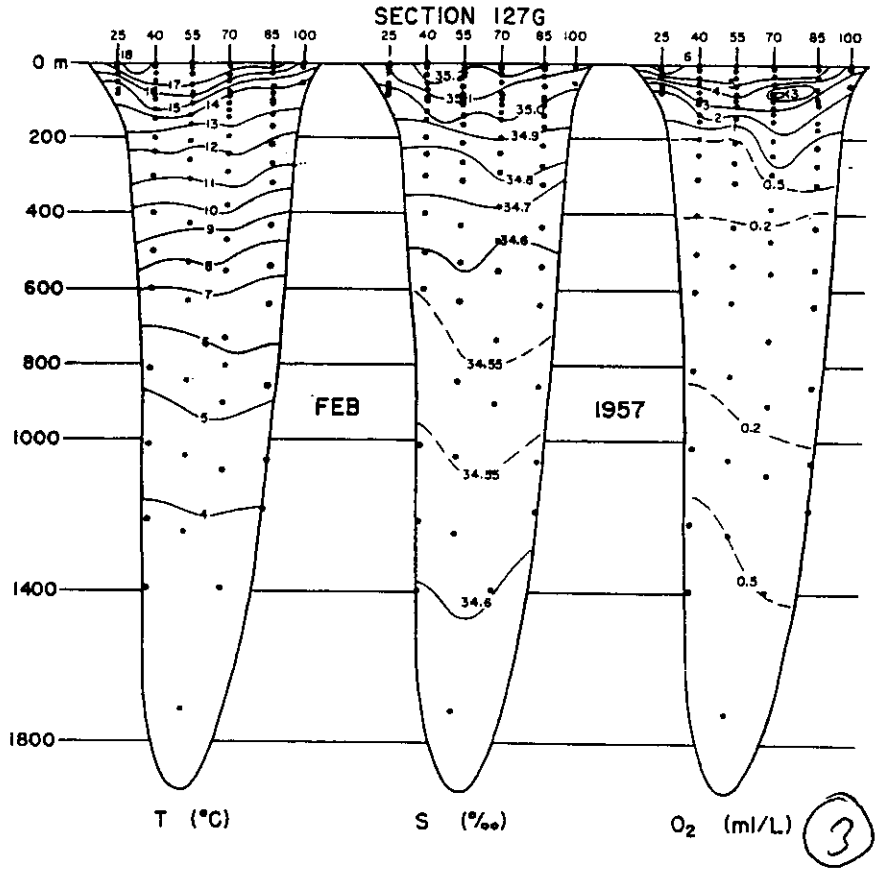
SECTION 127G
25 40 55 70 85 100
0 m
200
400
600
800
1000
1400
1800
FEB
1957
T (°C)
S (‰)
O2 (ml/L)

3

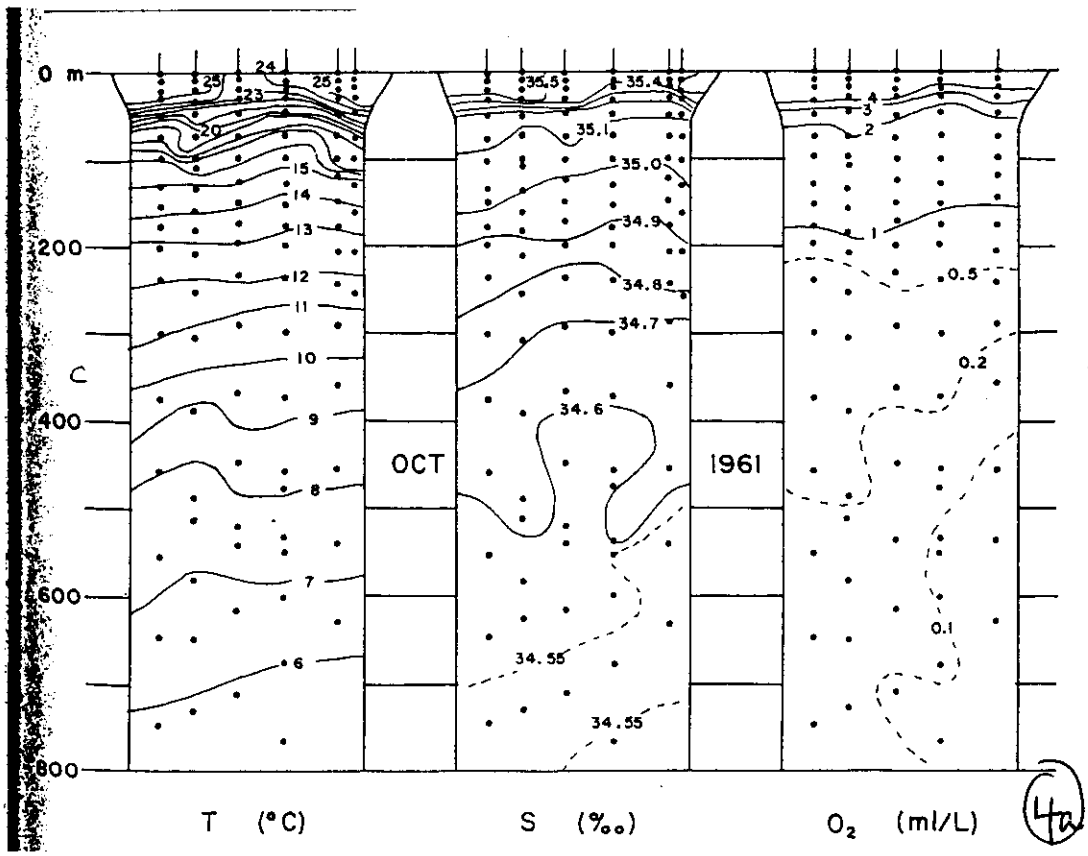
0 m
200
400
600
800
OCT
1961
T (°C)
S (‰)
O2 (ml/L)

4a

GC 3, 4a

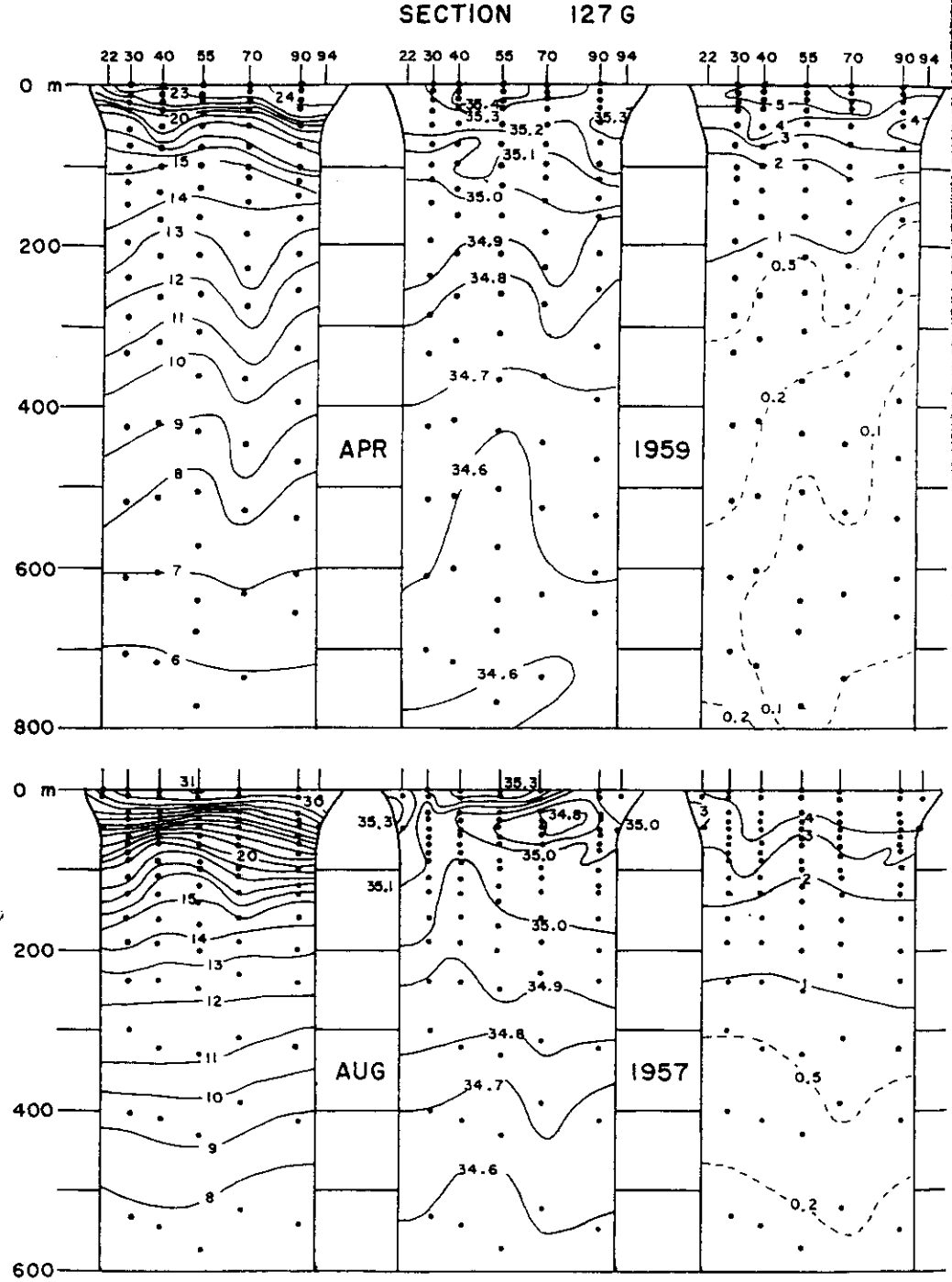

FIG. 11.—Distribution of temperature, salinity, and dissolved oxygen

Mar 85/39

Apr 57

May 84

50

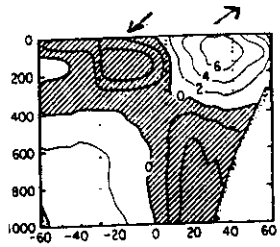

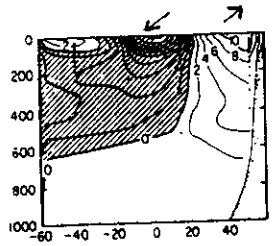

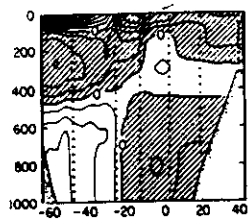

50

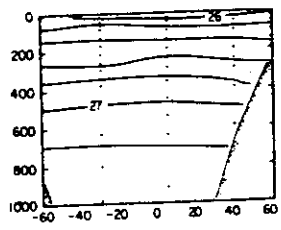

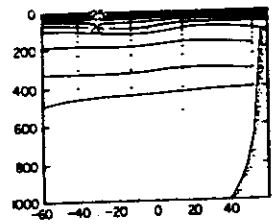

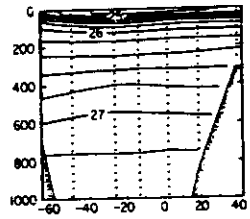

Jun 57

Aug 57

Oct 74

Nov 87

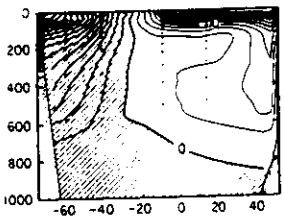

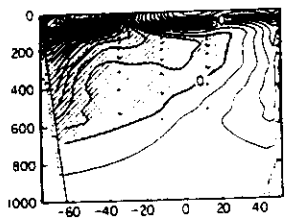

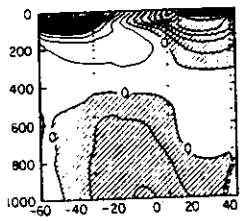

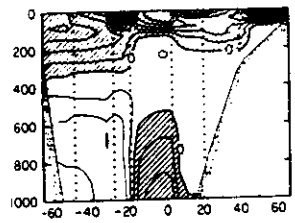

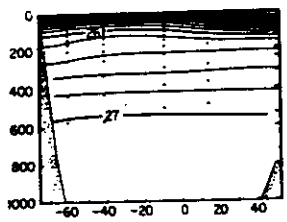

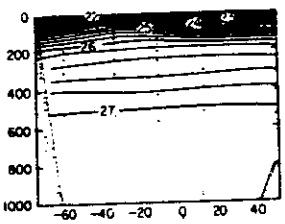

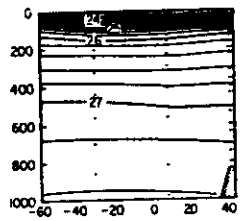

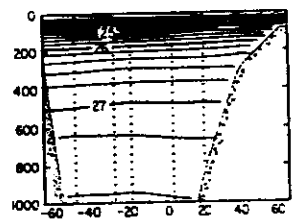

GC 5

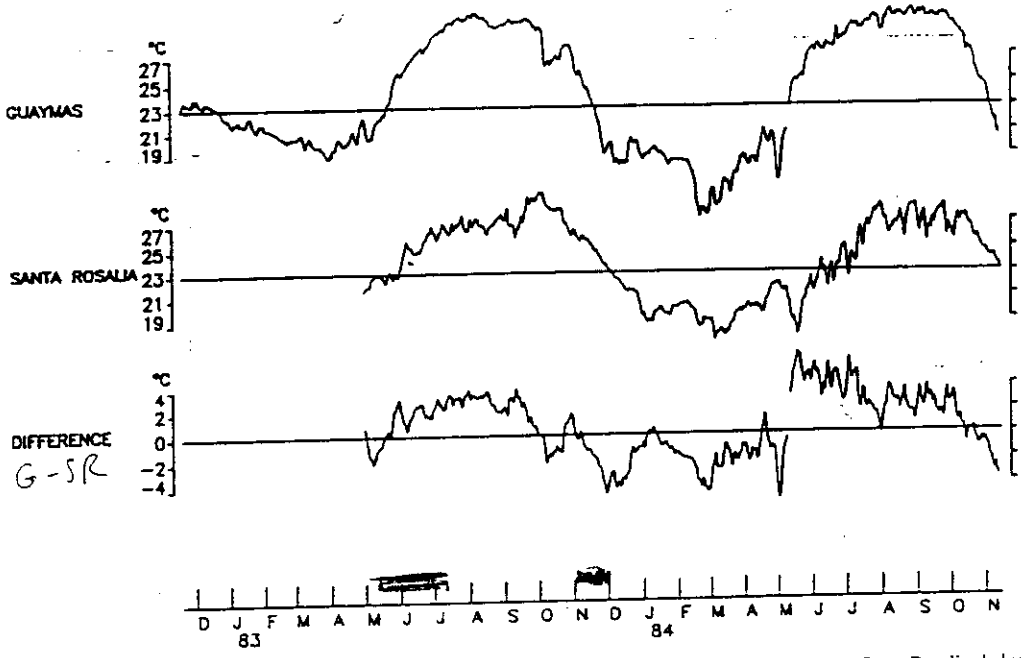

Fig. 7. Subinertial temperature measured 10 m below the surface at midshelf locations on the Guaymas and Santa Rosalia shelves and the difference between the two series.

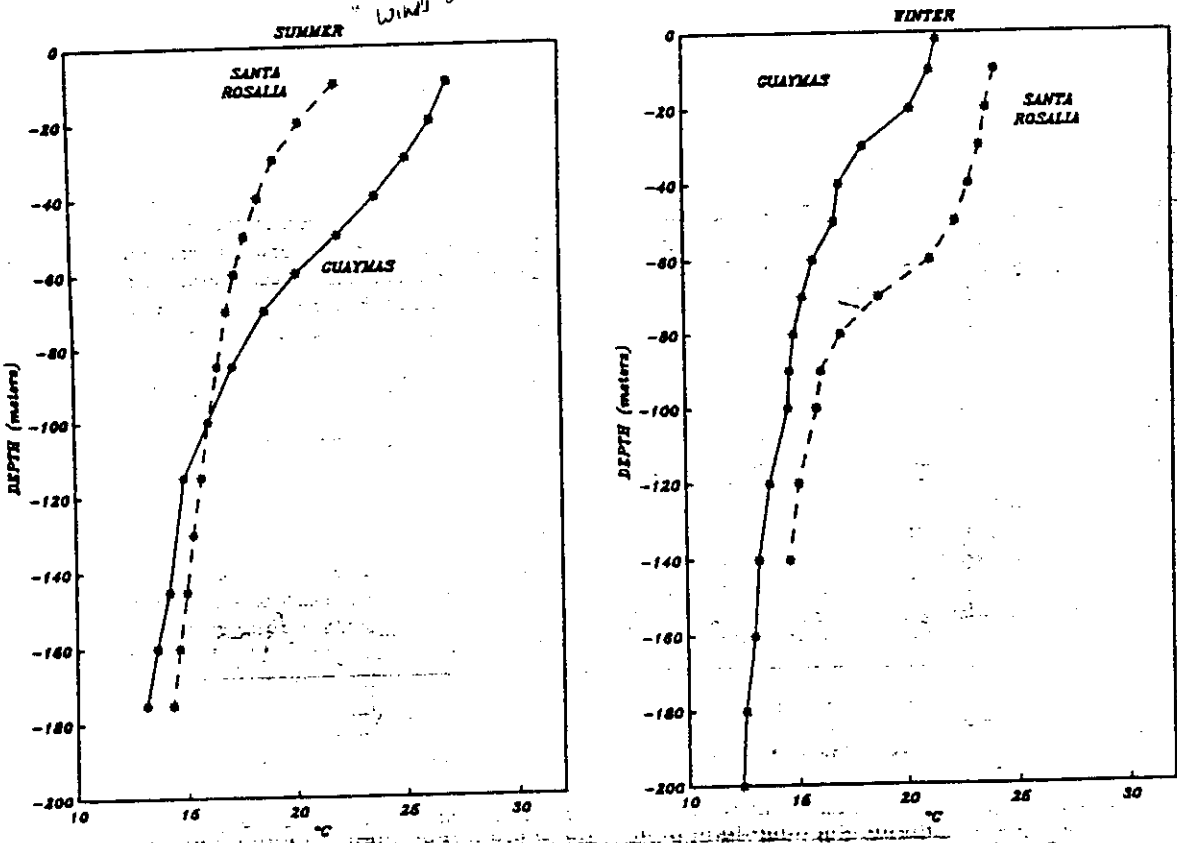

Fig. 8. Vertical temperature profiles at Guaymas (solid lines) and Santa Rosalia (dashed lines) for summer and winter. Summer values are average temperatures from the 200-m thermistor chains at M8 and M10. Averages are formed during the common time period May 11 to July 8, 1984. The winter profile at Guaymas is the average temperature at M8 during November 1984; the profile at Santa Rosalia is from a CTD cast made near M10 on November 14, 1984.

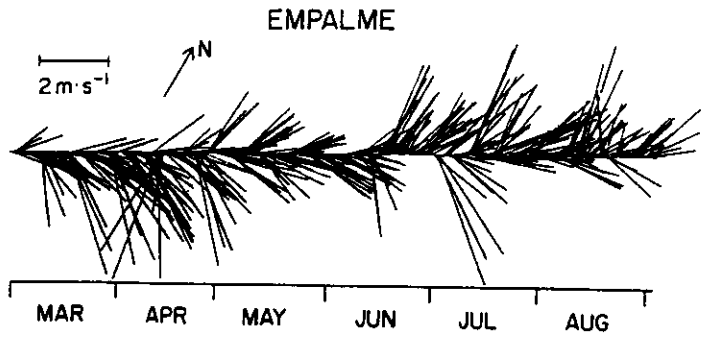

Figure 2

Time series of winds measured at a height of 1000 mb from radiosonde launches at Empalme during 1980. The vectors have been rotated so that the general orientation of the Gulf is vertical on the page.

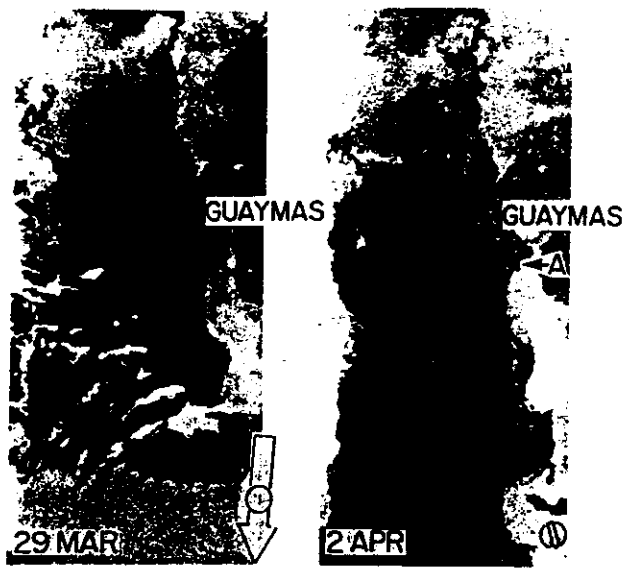

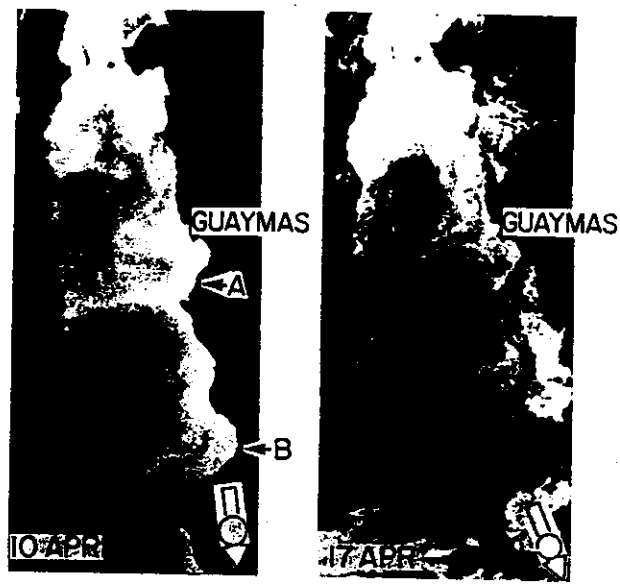

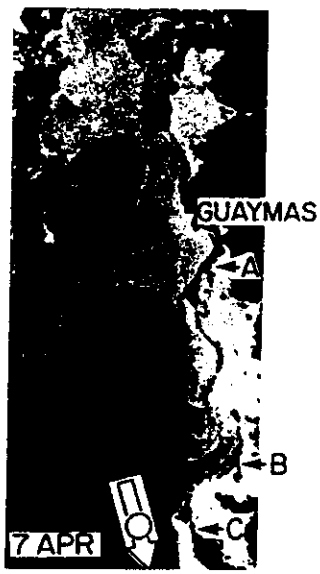

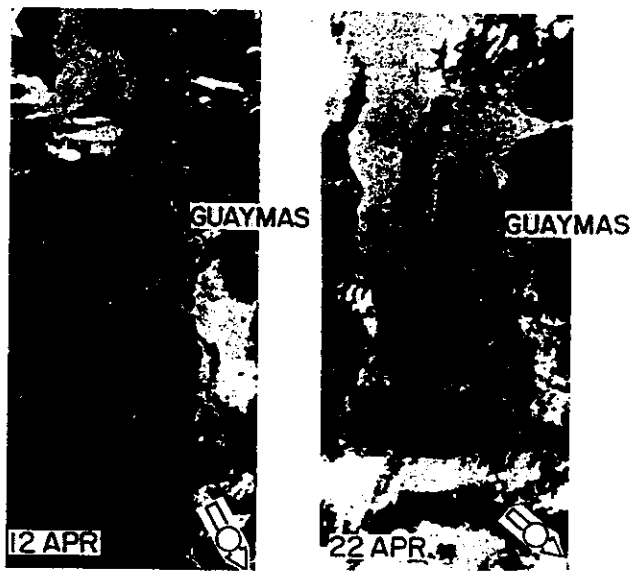

Figure 4

Sequence from March and April illustrating the temporal evolution of upwelling plumes off the east coast and the southward extension of the Ballenas Channel fronts. In this and subsequent figures, the arrows indicate the wind averaged from the two radiosoundings taken on that day. The diameter of the circle in the arrow provides the scale of 1 m. s⁻¹.

GC 7

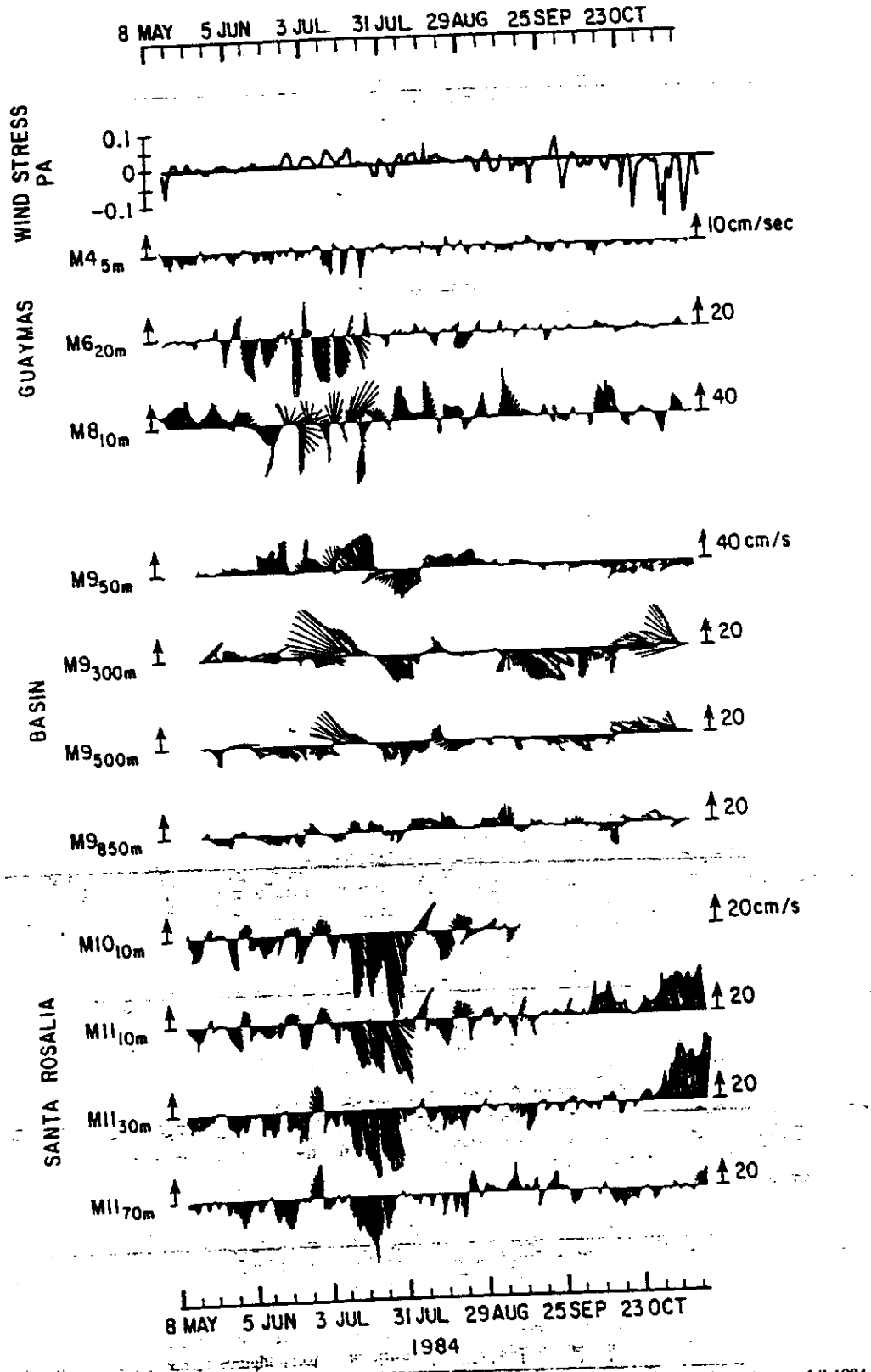

Fig. 19. Low-frequency vector time series of currents across the Guaymas–Santa Rosalia transect during the summer–fall 1984 deployment versus wind stress. A vector pointing up the page corresponds to upgulf flow.

GC 8

TABLE 4. Correlations, as in Table 2, for Alongshelf Currents During the Four Instrument Deployments

	Instrument Location	Correlation	Maximum Correlation	Lag, days
		November 1982 to May 1983		
GY	$M7_{10m} - M7_{70m}$	0.82*		0.0
		May–November 1983		
GY-TO	$M1_{70m} - M7_{70m}$	0.49*	0.60*	1.1
GY-SR	$M7_{70m} - M11_{65m}$	-0.28		0.0
		November 1983 to May 1984		
GY-SR	$M7_{70m} - M11_{10m}$	0.07		0.0
		May–November 1984		
GY	$M4_{5m} - M6_{20m}$	-0.14	0.51*	-2.2
	$M8_{10m} - M4_{5m}$	0.14	0.24*	1.0
	$M4_{4m} - M9_{50m}$	-0.26*		0.0
	$M6_{20m} - M8_{10m}$	0.35*	0.52*	1.3
SR	$M11_{11} - M11_{30m}$	0.86*		0.0
	$M11_{10m} - M11_{70m}$	0.34*		0.0
	$M11_{30m} - M11_{70m}$	0.55*		0.0
	$M10_{30m} - M11_{10m}$	0.94*		0.0
TO	$M1_{10m} - M1_{70m}$	0.78*		0.0
BA	$M9_{300m} - M9_{500m}$	0.90*		0.0
	$M9_{300m} - M9_{850m}$	0.41*		0.0
TO-GY	$M1_{10m} - M8_{10m}$	-0.08	0.30*	1.9
GY-BA	$M6_{20m} - M9_{50m}$	-0.15	-0.46*	3.3
	$M8_{10m} - M9_{50m}$	-0.48*	-0.53*	1.0
BA-SR	$M9_{50m} - M11_{10m}$	-0.54*	-0.65*	2.7
	$M9_{50m} - M11_{30m}$	-0.55*	2.1	

Stations are TO, Topolobampo; GY, Guaymas; BA, Guaymas Basin; SR, Santa Rosalia.
* Above 95% significance.

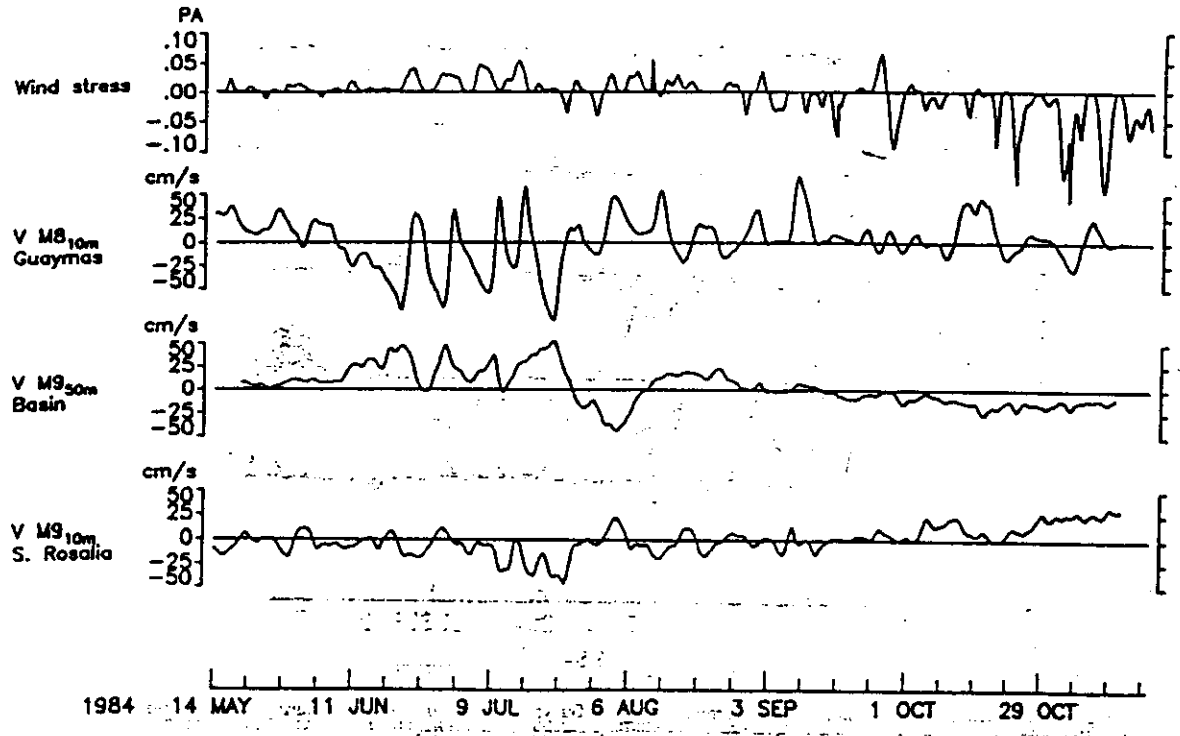

Fig. 20. Comparison of alongshelf currents in the basin, on the Guaymas and Santa Rosalia shelves, and wind stress during the summer–fall 1984 deployment.

GC 9

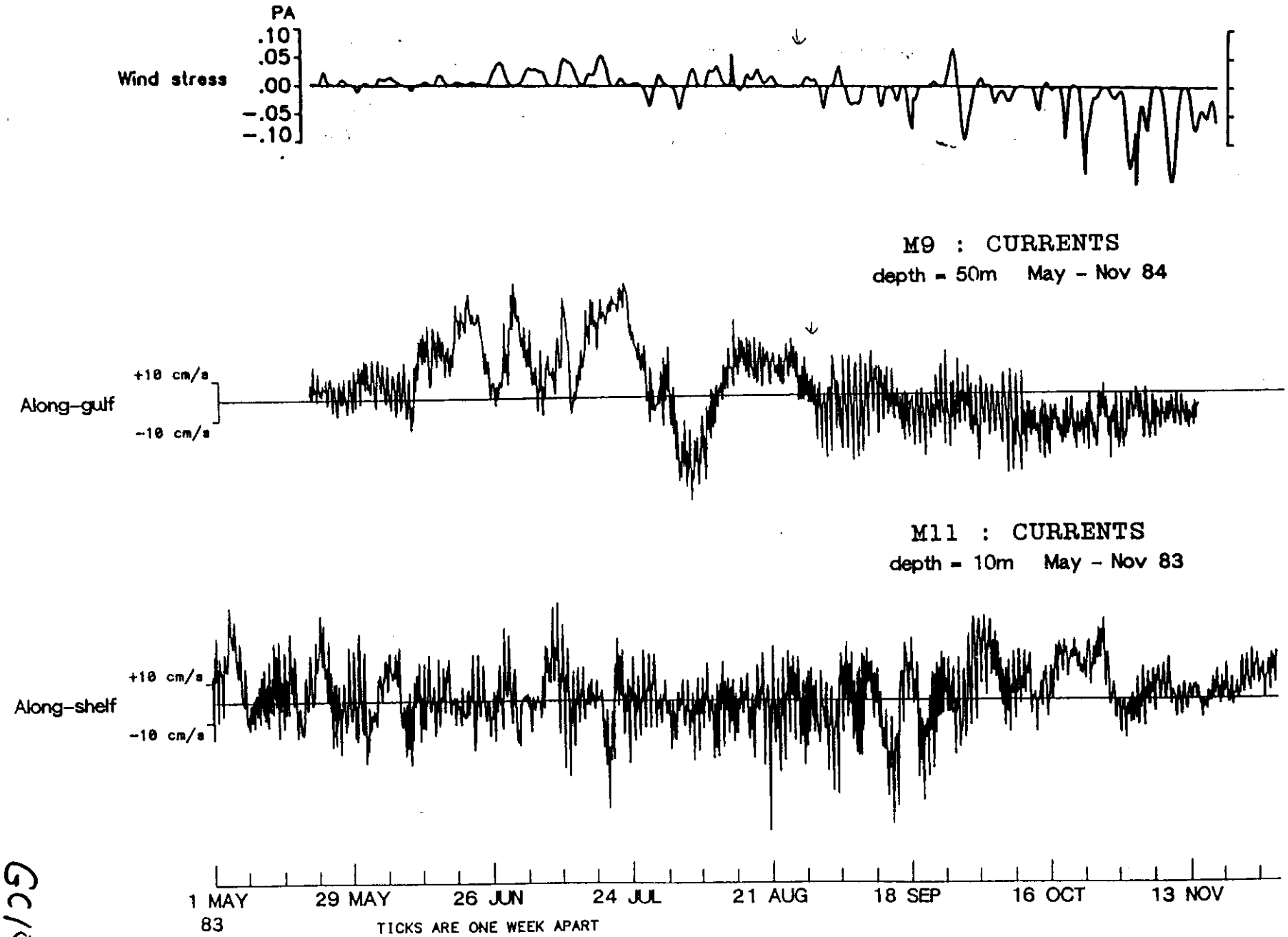
PA
.10
.05
.00
-.05
-.10
Wind stress
M9 : CURRENTS
depth = 50m May - Nov 84
+10 cm/s
-10 cm/s
Along-gulf
M11 : CURRENTS
depth = 10m May - Nov 83
+10 cm/s
-10 cm/s
Along-shelf
1 MAY
83
29 MAY
26 JUN
24 JUL
21 AUG
18 SEP
16 OCT
13 NOV
TICKS ARE ONE WEEK APART

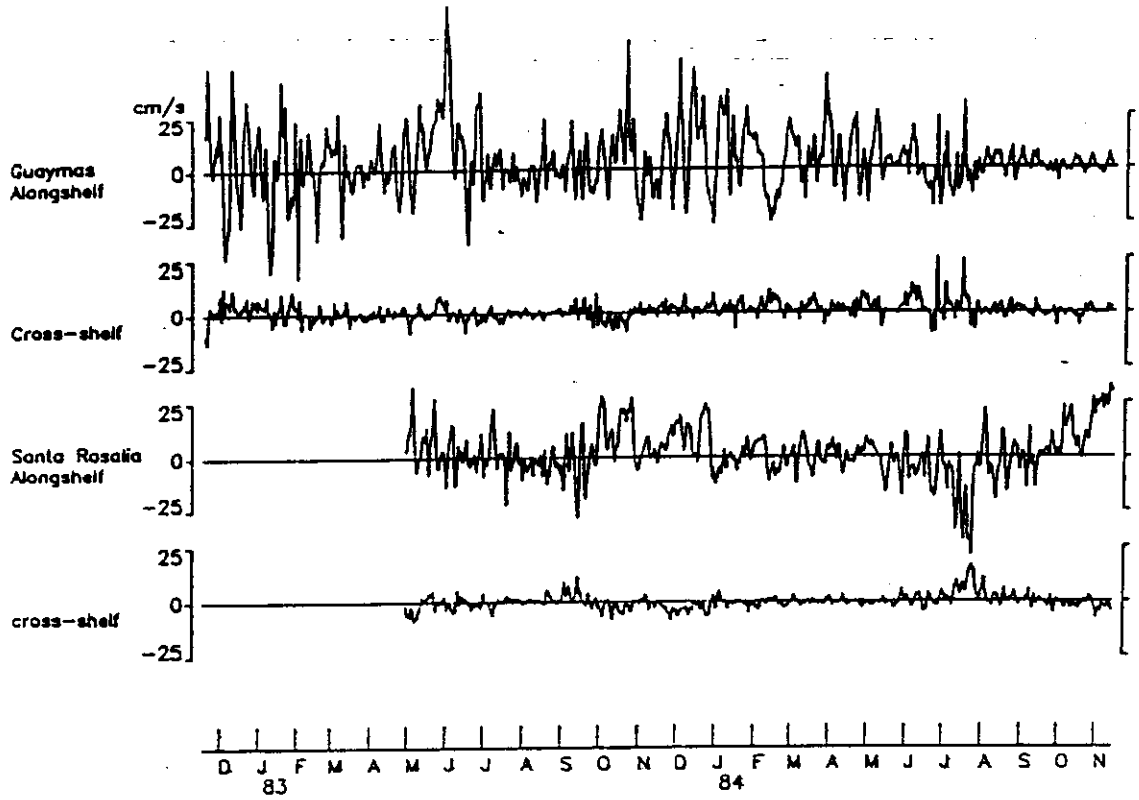

Fig. 17. Low-frequency currents at Santa Rosalia ($M11_{10m}$) and Guaymas ($M7_{10}$ from November 1982 to April 1983, $M7_{75m}$ from May–August 1983, $M7_{10m}$ from September–October 1983, $M7_{70m}$ from November 1983 to April 1984, and average between $M6_{20}$ and $M8_{10m}$ for May–November 1984).

GC 11

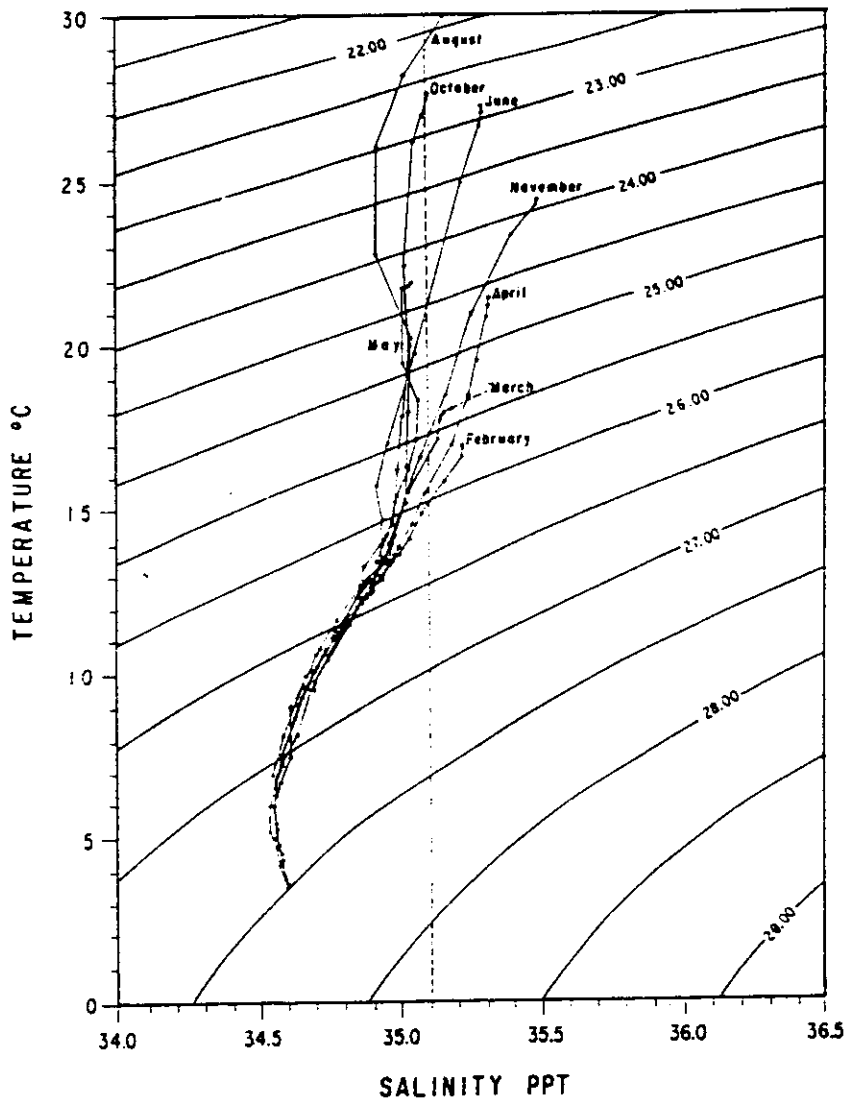

3. Mean monthly T–S seasonal cycle at the Guaymas Basin from all T–S data in Fig. 2.

BC 12a

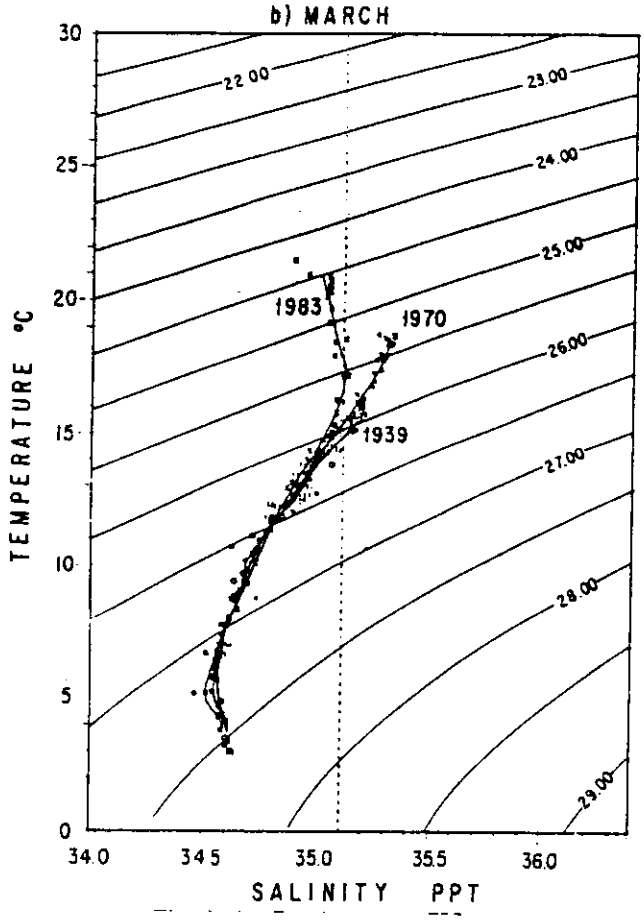
b) MARCH
TEMPERATURE °C
SALINITY PPT
1983
1970
1939
22.00
23.00
24.00
25.00
26.00
27.00
28.00
29.00
30
25
20
15
10
5
0
34.0
34.5
35.0
35.5
36.0

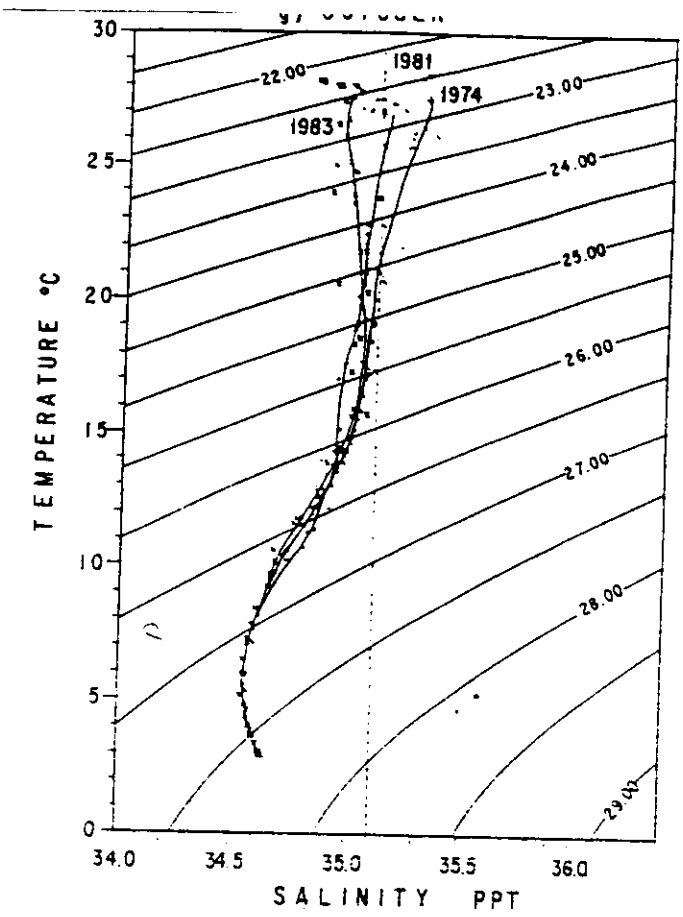
TEMPERATURE °C
SALINITY PPT
1981
1974
1983
22.00
23.00
24.00
25.00
26.00
27.00
28.00
29.00
30
25
20
15
10
5
0
34.0
34.5
35.0
35.5
36.0

GC 12bc

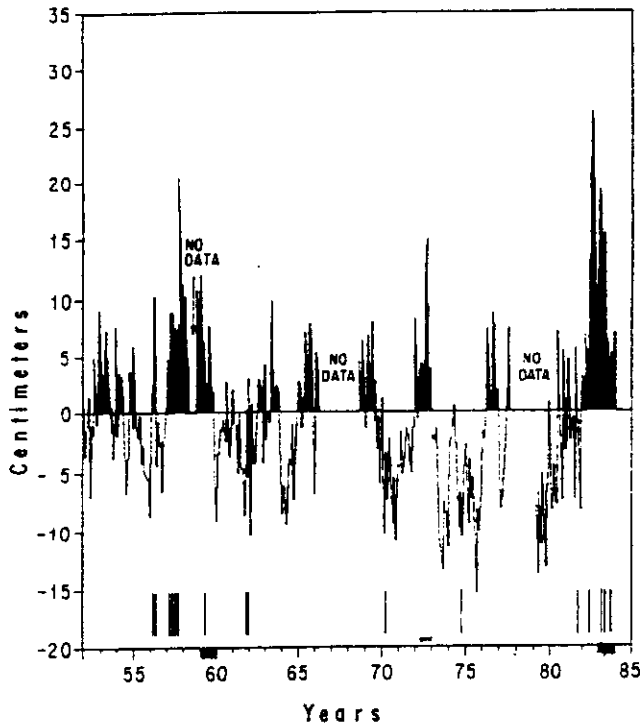

Fig. 5. Monthly sea level anomalies at Guaymas for the period 1952–1984. Positive values indicating episodes of El Niño are shaded. Solid lines on the time axis denote cruises from Table 1, when hydrographic data were collected at the Guaymas Basin.

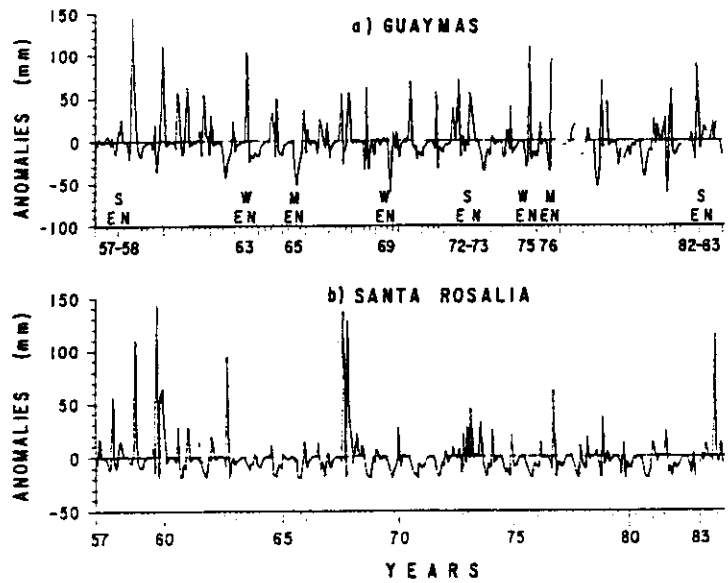

Fig. 7. Monthly rain anomalies (MRA) at (a) Guaymas and (b) Santa Rosalia for the period 1957–1983. El Niño years (EN) and their intensity (S=strong, M=moderate and W=weak) after QUINN *et al.* (1978) are also shown.

GCIX
IX

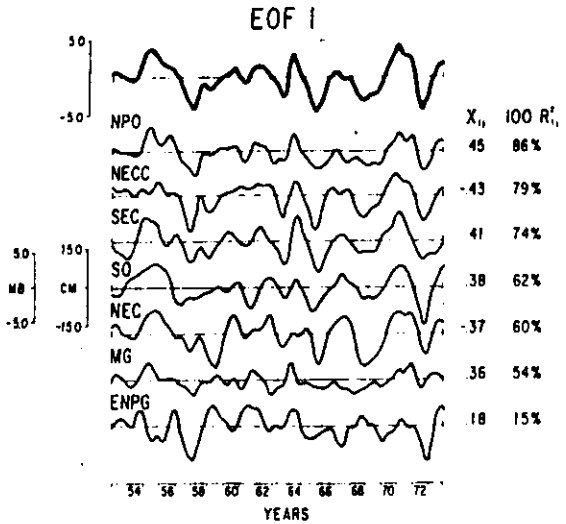

Figure 5. Time series of first eigenfunction of remote variables plotted at top of figure. Vertical scale for eigenfunction in units of the total normalized variance. Original series arranged below according to their percent contribution ($100R^2_{ij}$) to this EOF. Series with negative eigenvector elements (X_{ij}) are inverted to agree with sense of variance in the EOF. Variances of original series plotted here are not normalized; units given in cm and mb. Only those series contributing more than 10% of their variance to this EOF are shown.

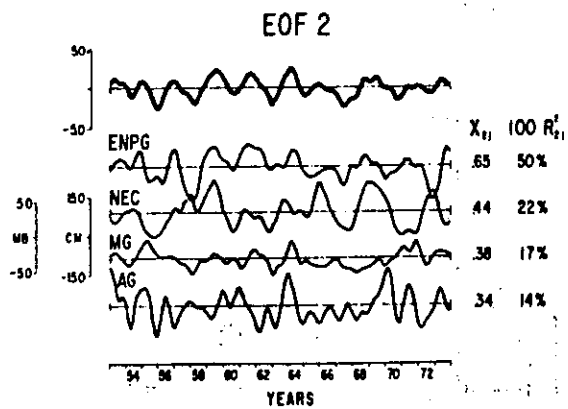

Figure 6. Time series of second eigenfunction of remote climatic variables plotted at top of figure. Original series arranged as in Figure 5.

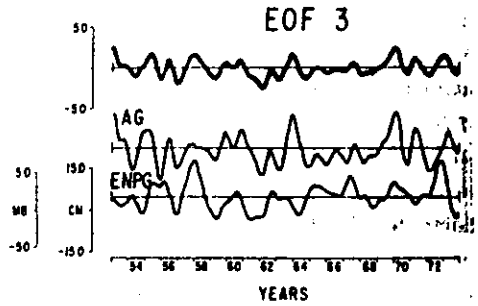

Figure 7. Time series of third eigenfunction of remote climatic variables plotted at top of figure. Original series arranged as in Figure 5.

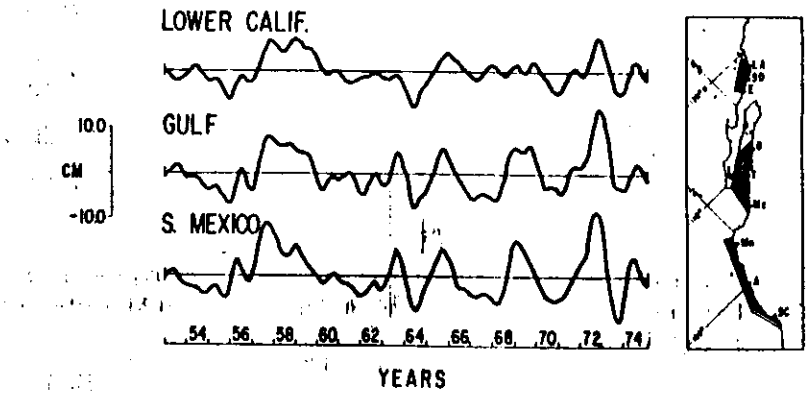

Figure 9. Filtered monthly sea level anomalies from the Gulf of California compared to regional averages of coastal sea level off southern México and lower California. Location of stations used to compute regional averages are shown on inset map. (LA: Los Angeles; SD: San Diego; E: Ensenada; G: Guaymas; T: Topolobampo; LP: La Paz; Mz: Mazatlán; Mn: Manzanillo; A: Acapulco; Sc: Salinacruz).

Table 2. Correlations (r) between first 3 EOF's of the remote variables and regional sea level and shore temperature in the Gulf of California and with regional sea levels off the coast of southern México and lower California. Significances ≥90% are shown in parenthesis below the correlation coefficients.

	EOF 1	EOF 2	EOF 3
Gulf of California Sea level	−.72 (>99.9)	.15	.24
Gulf of California Temperature	−.49 (>99.0)	−.04	−.15
Southern México Sea level	−.74 (>99.9)	.06	.19
Lower California Sea level	−.71 (>99.9)	−.02	.13

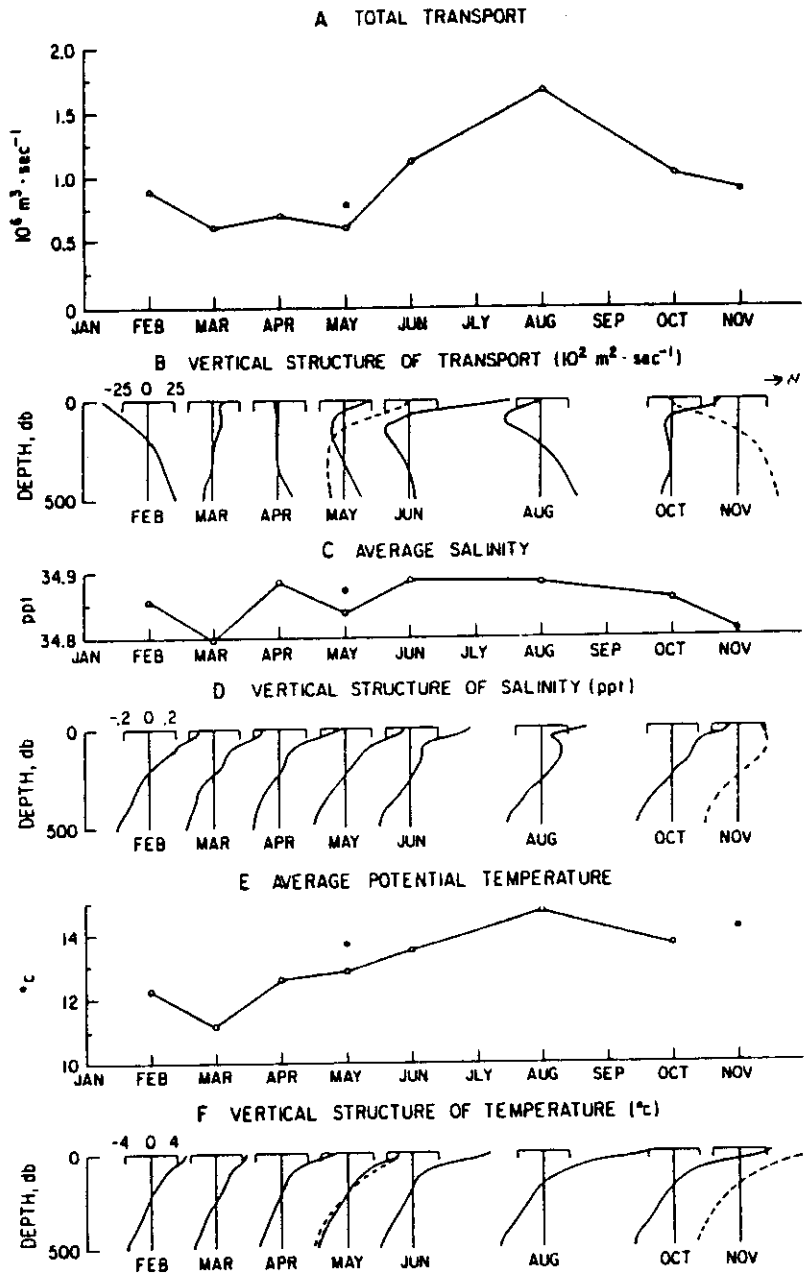

Fig. 17. Transport, salinity and temperature across line 50 (Guaymas to Santa Rosalia). For each variable, the average value over the top 500 m is plotted as a function of time (Figures 17*a*, 17*c* and 17*e* for transport, salinity and temperature, respectively). Also shown is the vertical structure of each variable over the top 500 m as a function of time (Figures 17*b*, 17*d*, and 17*f*). In Figures 17*d* and 17*f* the average value has been subtracted, to emphasize changes in vertical structure. Dashed curves and solid dots represent 1983 (ENSO year) cruises.

GC 15

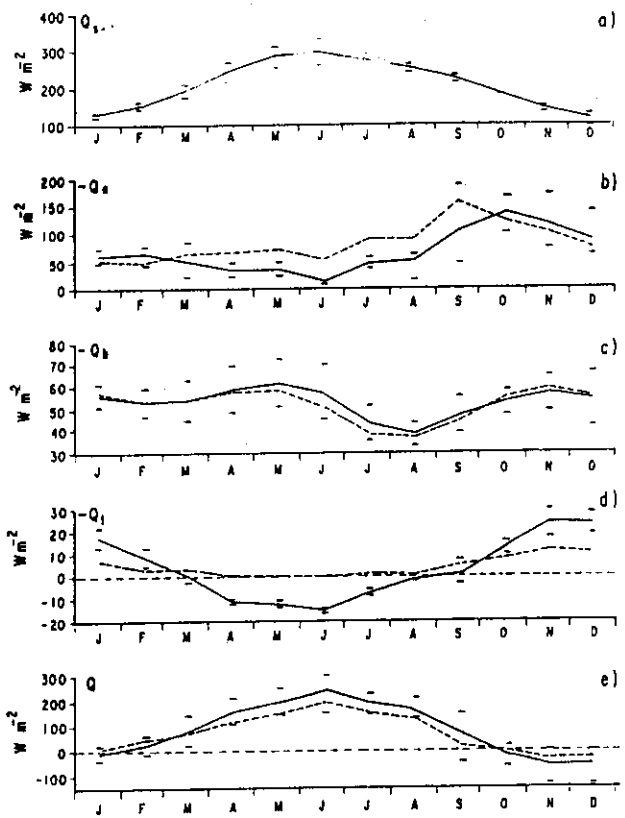

Fig. 2. The seasonal cycle of surface heat fluxes, with the effect of climatic variability: Dotted line, with coastal sea surface temperature. Solid line, with sea surface temperature from hydrographic stations with bottom depth ≥100 m. The variability bars correspond to the latter. (a) Net shortwave radiation, (b) latent heat flux, (c) net longwave radiation, (d) sensible heat flux, and (e) total heat flux.

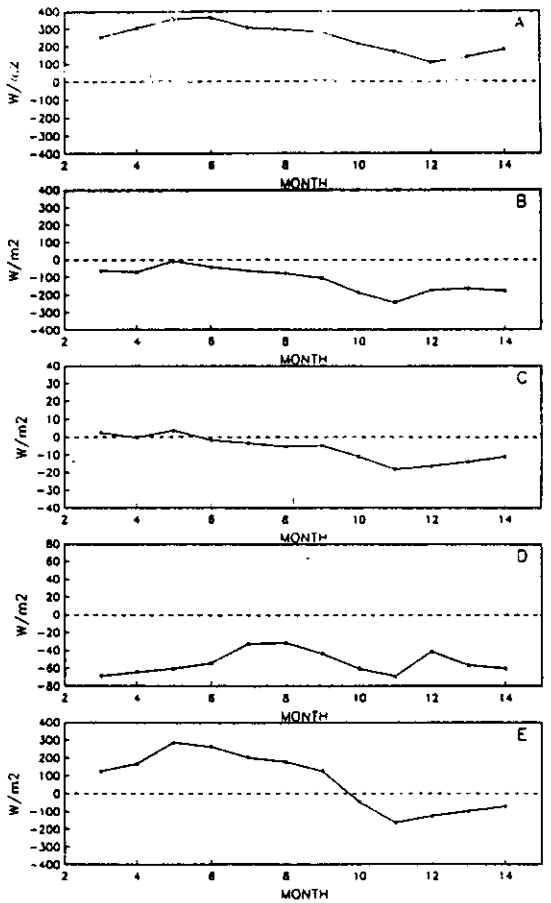

Average monthly surface fluxes for the region north of Guaymas-Santa Rosalia line: A) incident solar radiation, B) latent heat flux, C) sensible heat flux, D) long-wave radiation, E) total net surface heat flux.

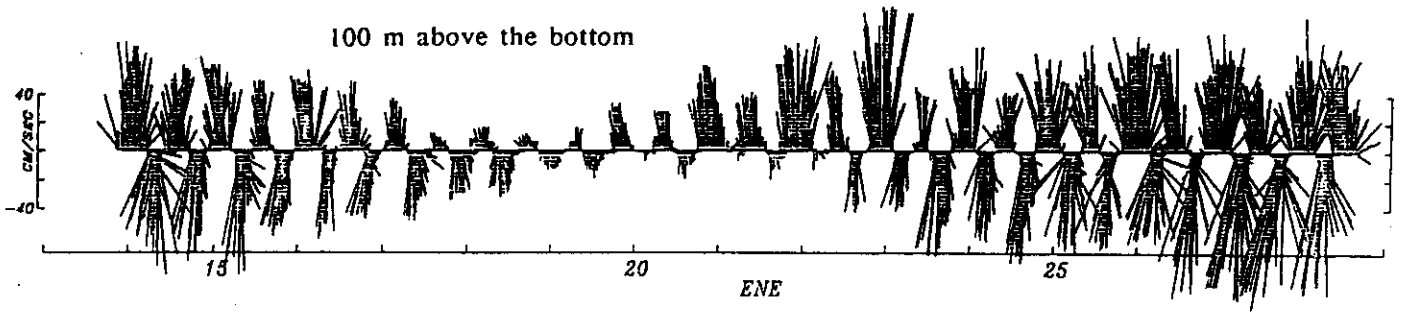

North sill, Ballenas Channel (H = 605 m)

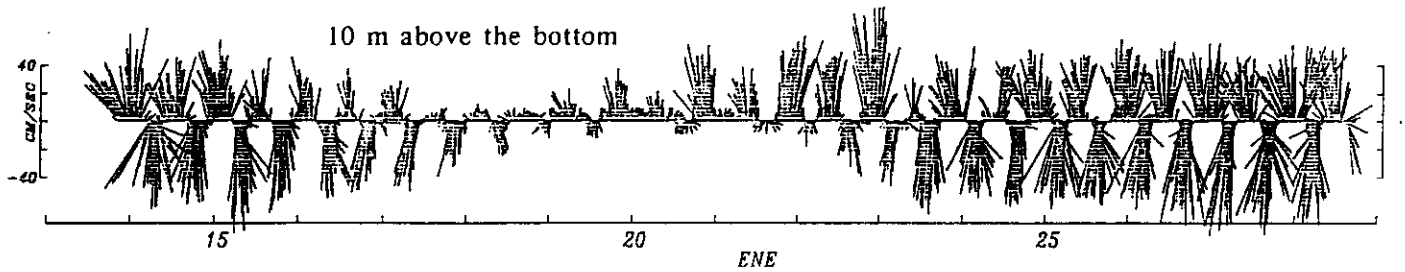

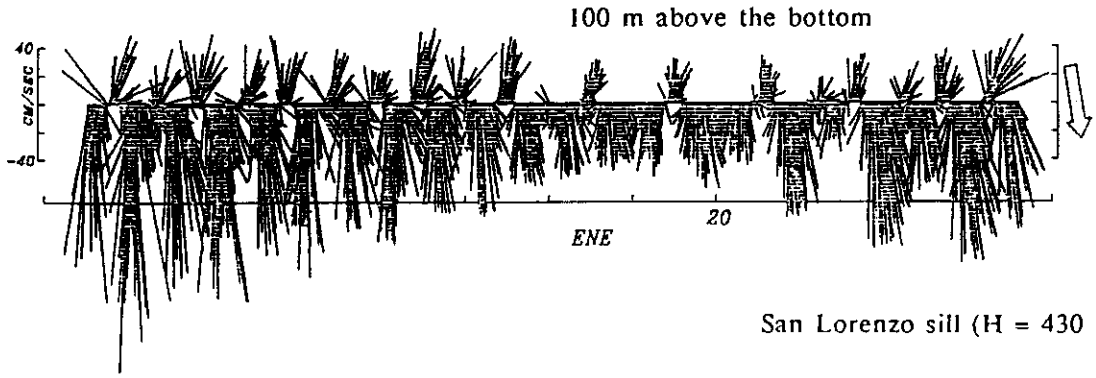

San Lorenzo sill (H = 430 m)

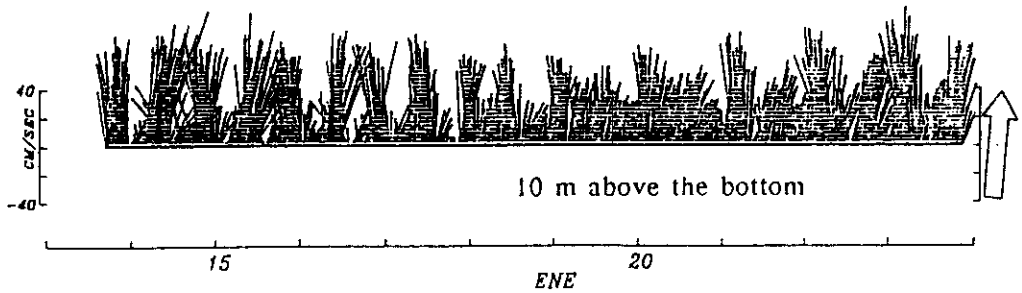

GC 17

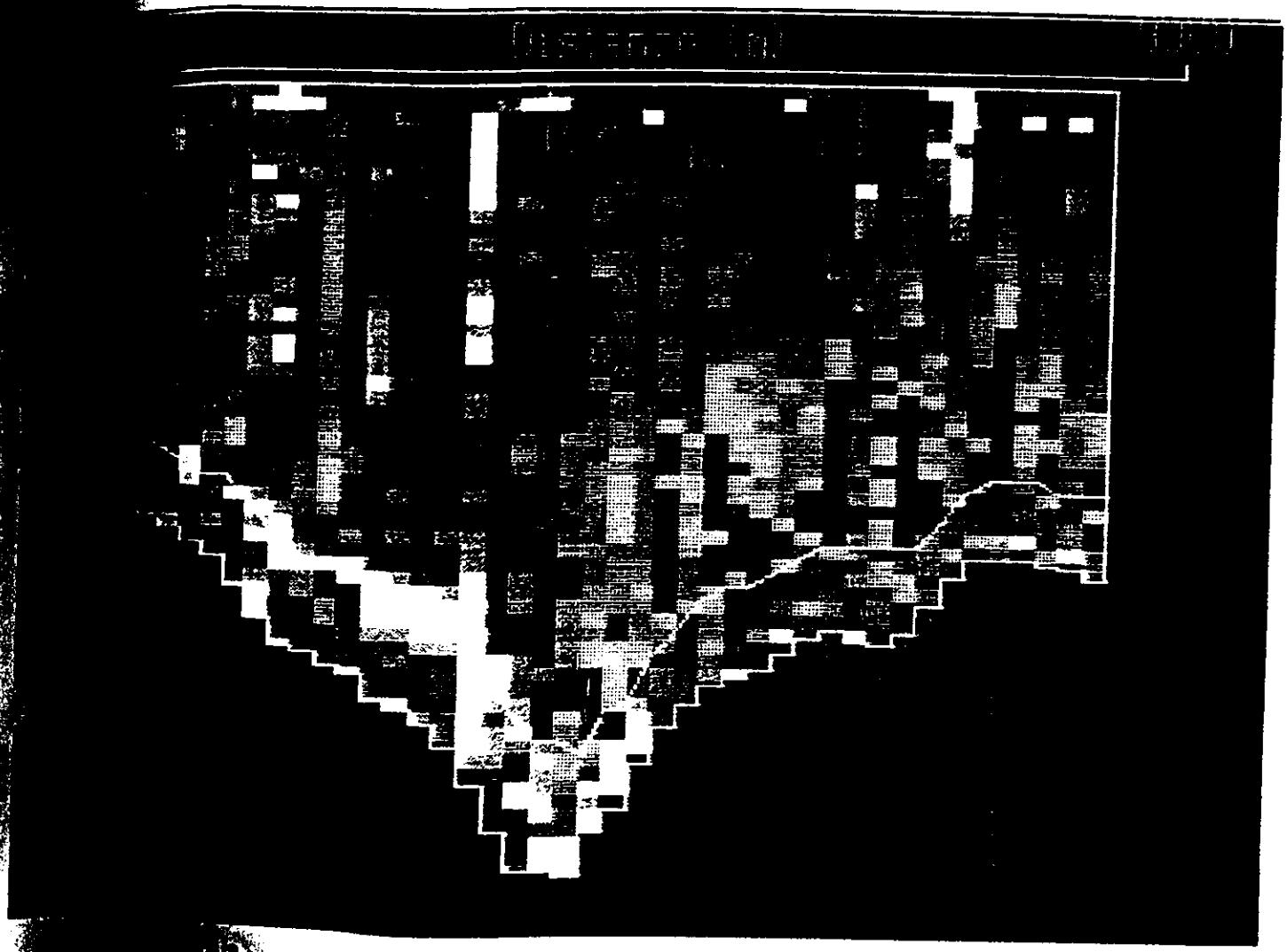

San Lorenzo sill

San Lorenzo spur

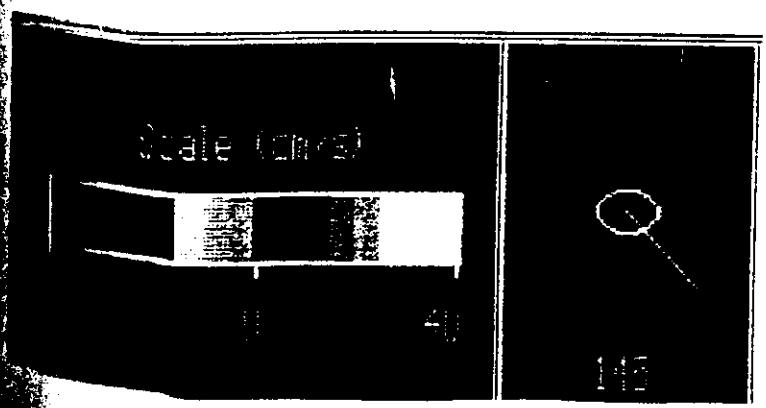

GC18

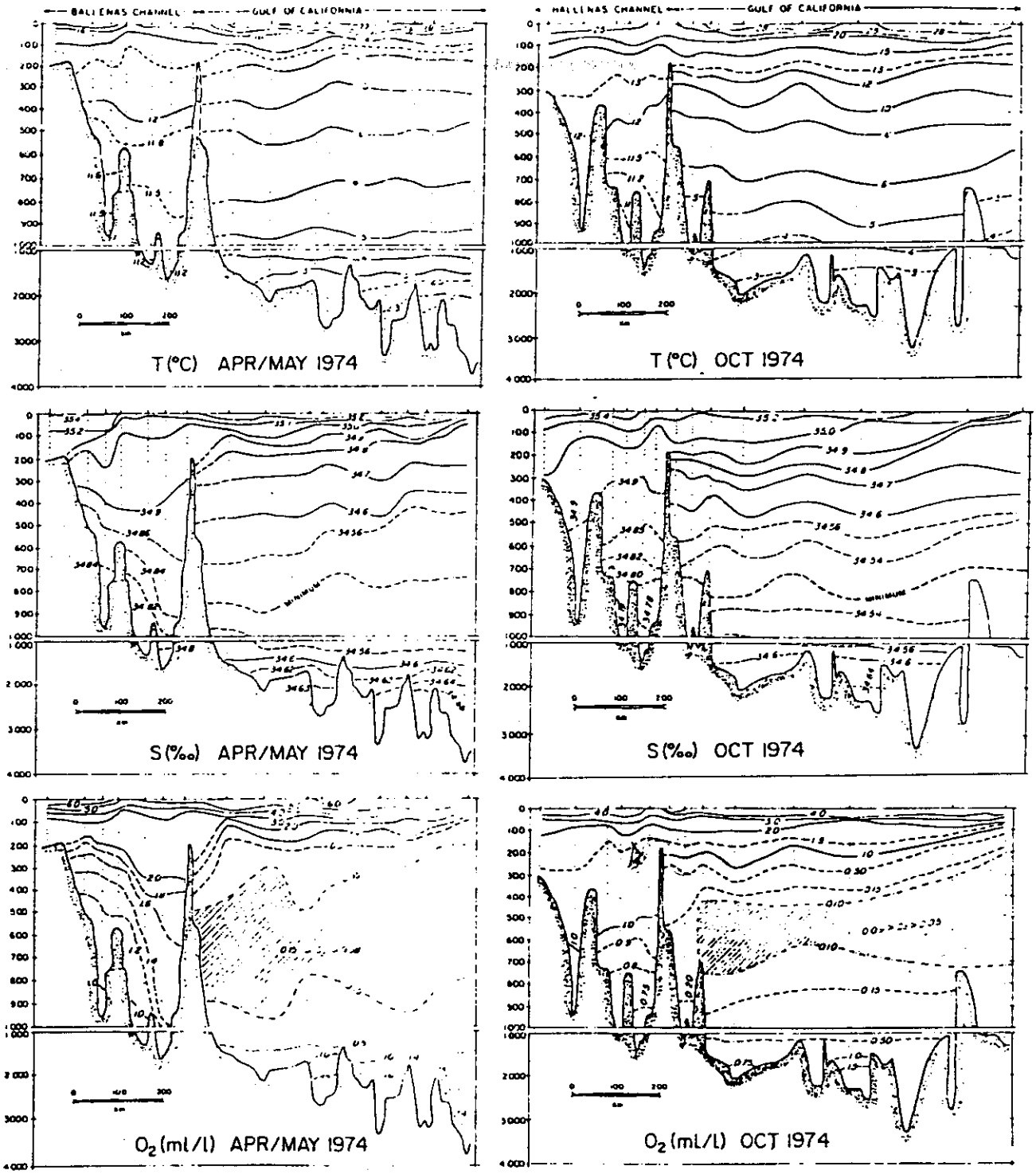
BALLENAS CHANNEL
GULF OF CALIFORNIA
T (°C) APR/MAY 1974
T (°C) OCT 1974
S (‰) APR/MAY 1974
S (‰) OCT 1974
O2 (ml/l) APR/MAY 1974
O2 (mL/L) OCT 1974
DEPTH IN METERS

GC 19

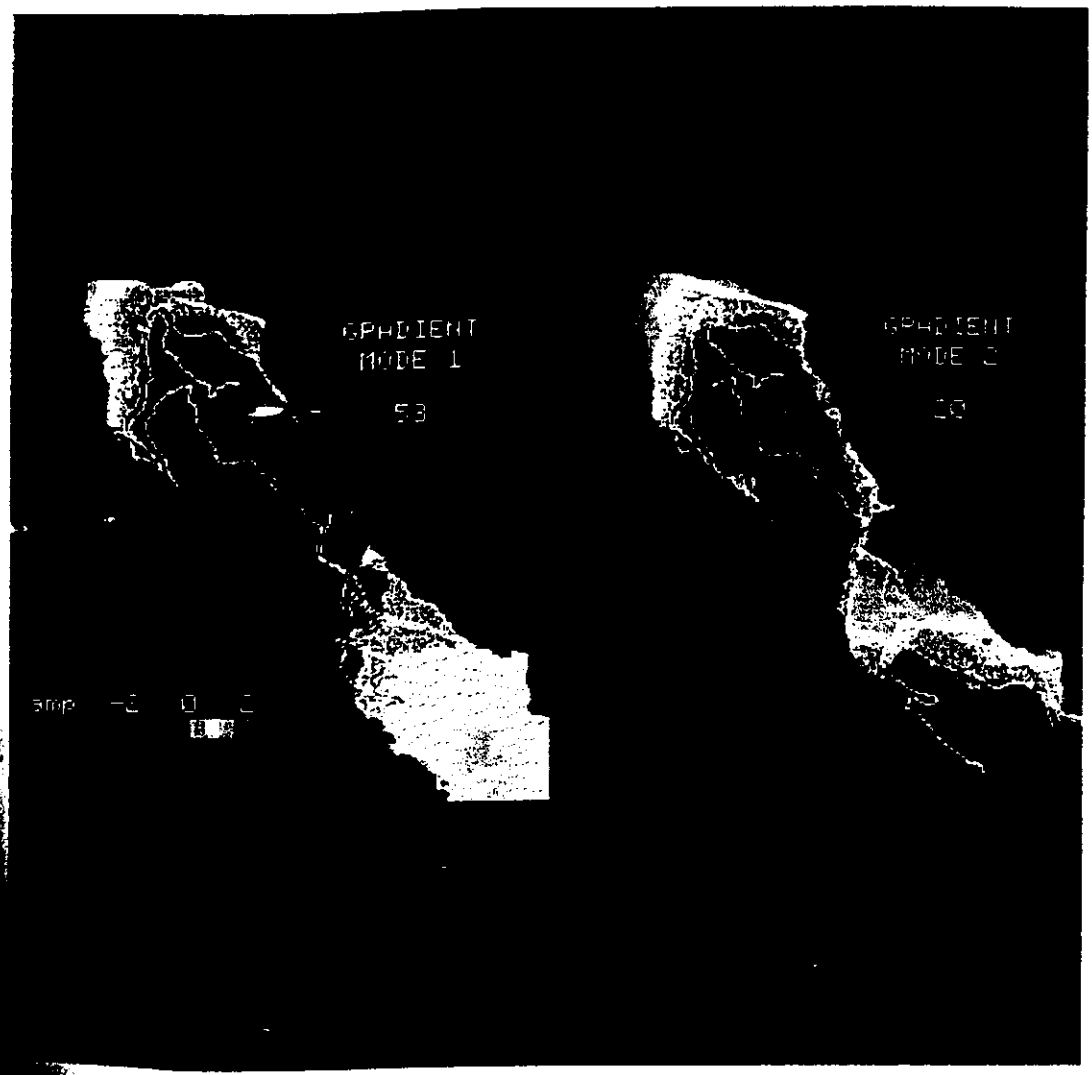

Fig. 14. Gradient EOF modes 1 and 2 with bathymetry.

GC 20

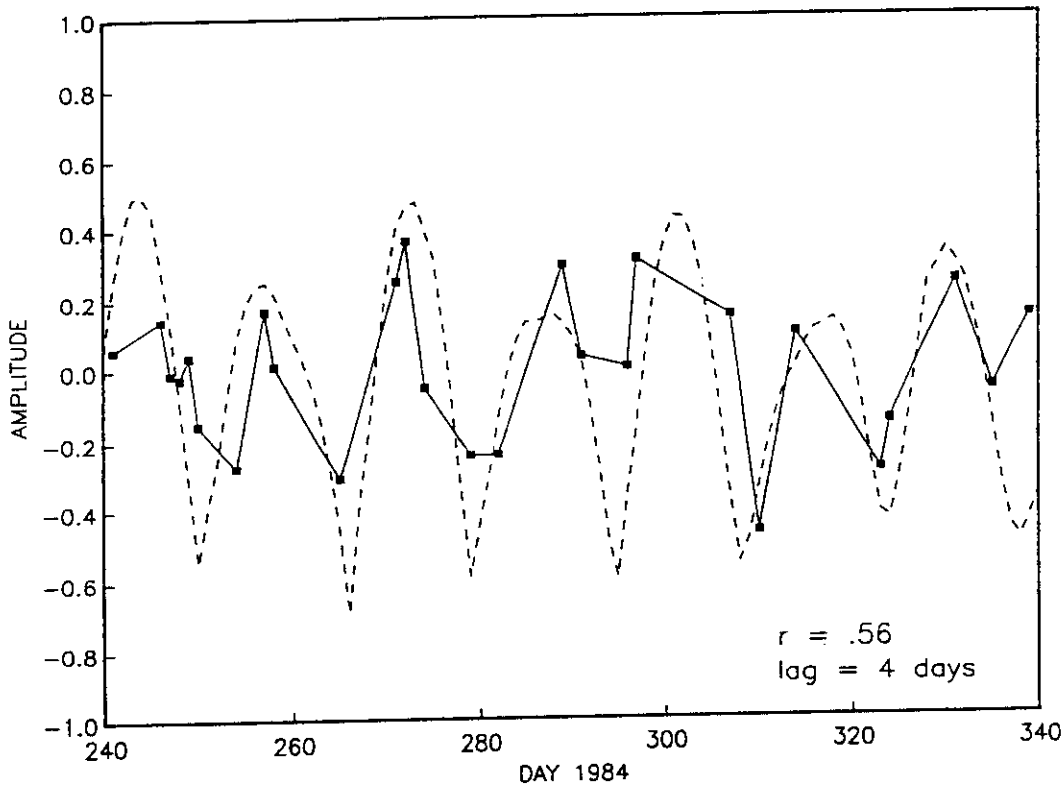

Figure 20. Comparison of the detrended gradient mode 1 amplitudes for individual images between 28 August 1984 and 4 December 1984 (solid line) and the maximum daily tidal range at Puerto Penasco (rescaled for plotting). Maximum correlation (r=0.56) occurs at a lag of 4 days, with the largest SST gradients occurring approximately 4 days after the largest tidal ranges.

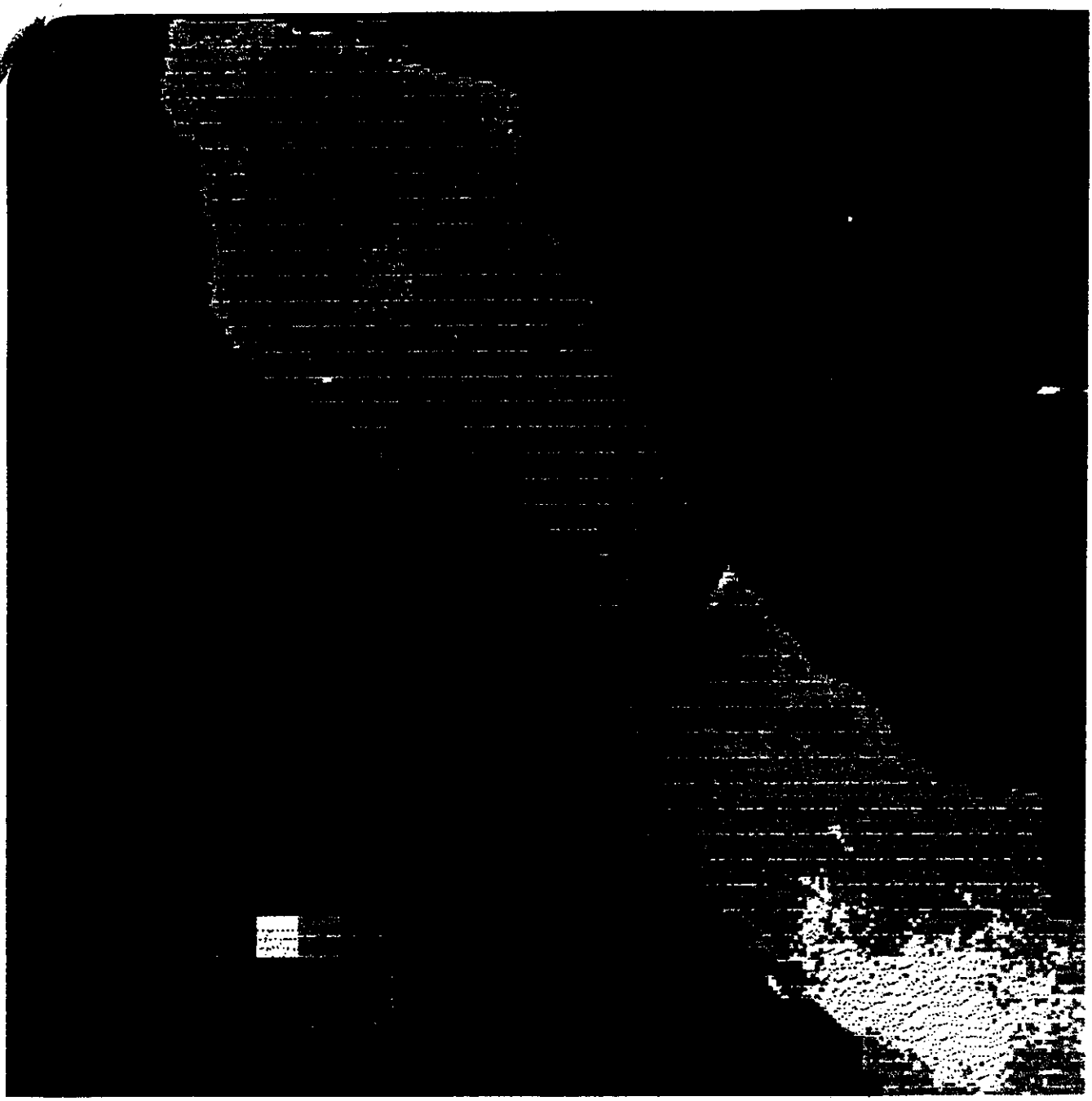

Figure 7. Spatial distribution of net surface heat flux (W/m2) for the northern Gulf of California.

GC22

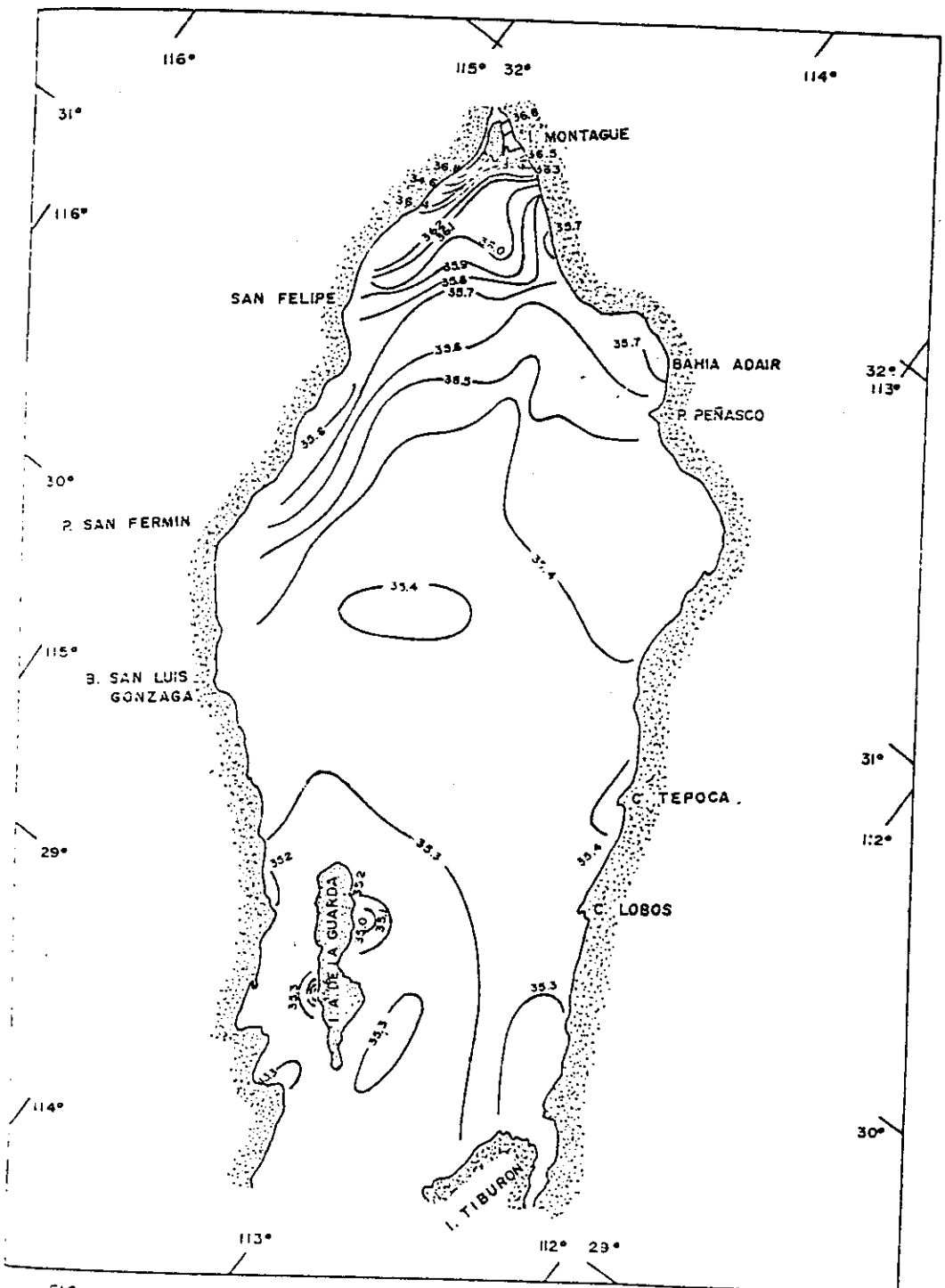

FIG. 10 DISTRIBUCION SUPERFICIAL DE SALINIDAD (‰) EN LA PARTE NORTE DEL GOLFO DE CALIFORNIA.

500

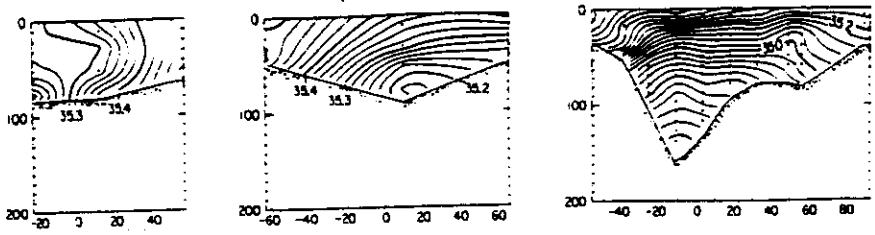

500

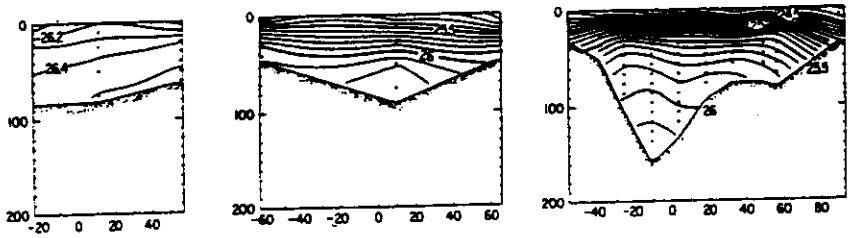

500

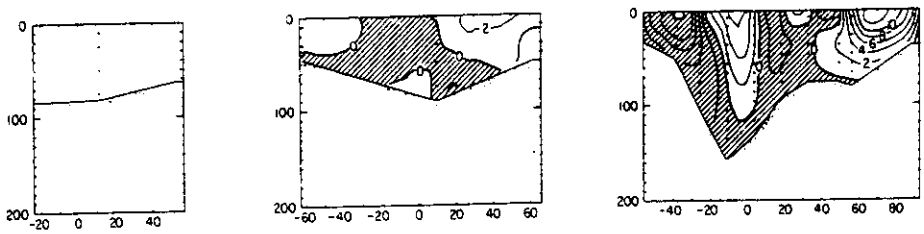

Jan 57 Aug 57 Oct 74 Nov 83

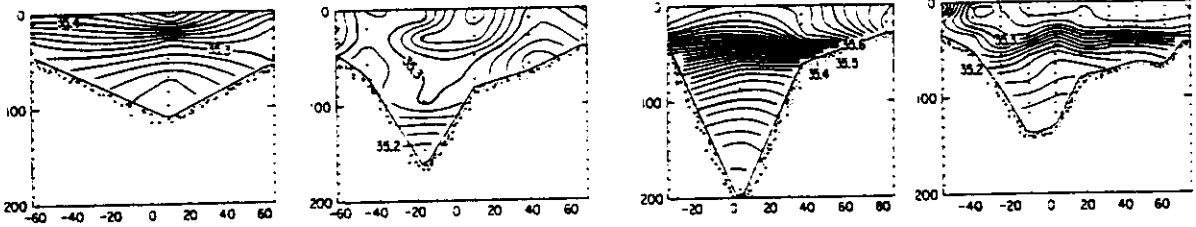

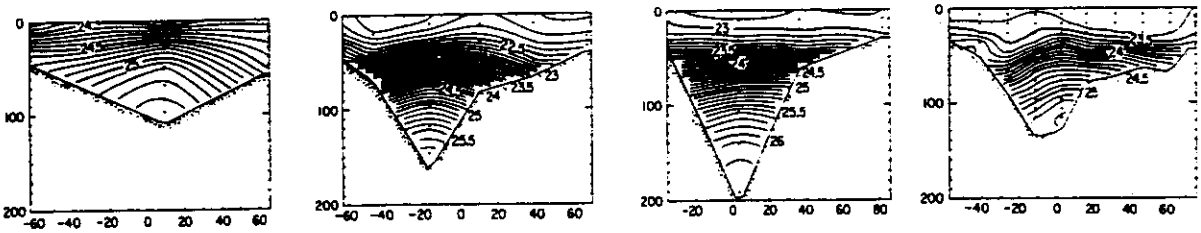

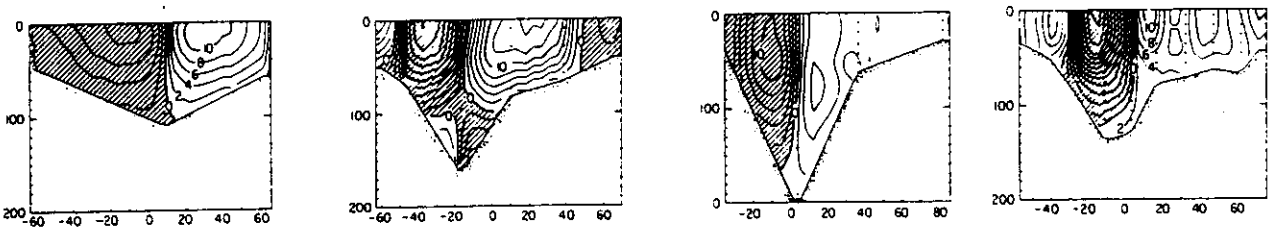

GC24

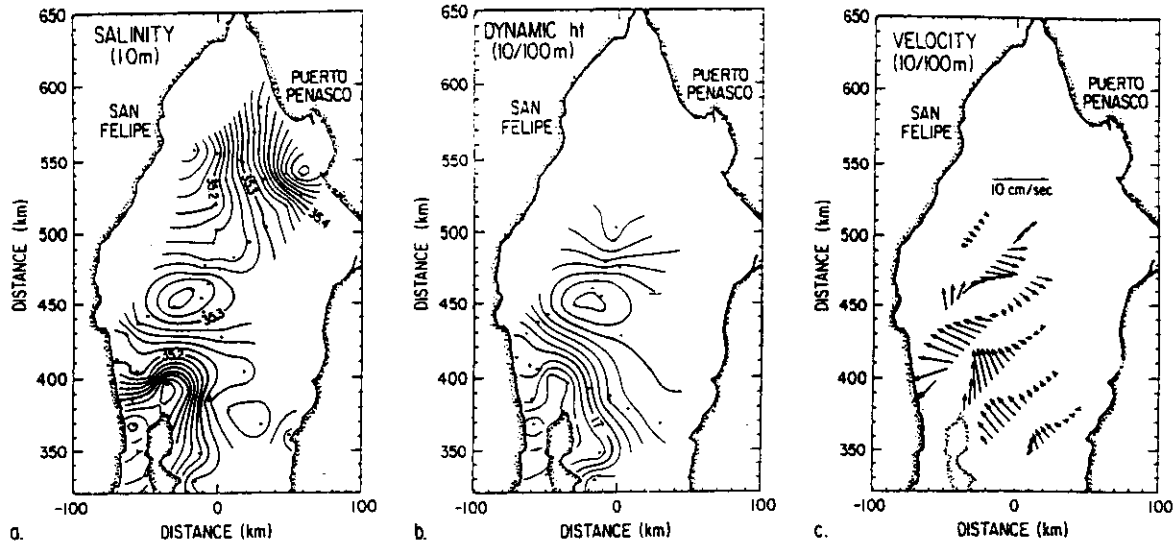

Fig. 15. The anticyclonic gyre found in the northern gulf in March 1985: (*a*) salinity at 10 m, (*b*) dynamic height at 10 m relative to 100 m, and (*c*) velocity vectors derived from the dynamic height field. Note the high-salinity water trapped within the gyre, well away from the high-salinity source near Puerto Peñasco. The low salinities at the northern end of the Ballenas Channel (at 400 km in the north-south coordinate) are presumably associated with strong vertical mixing.

25

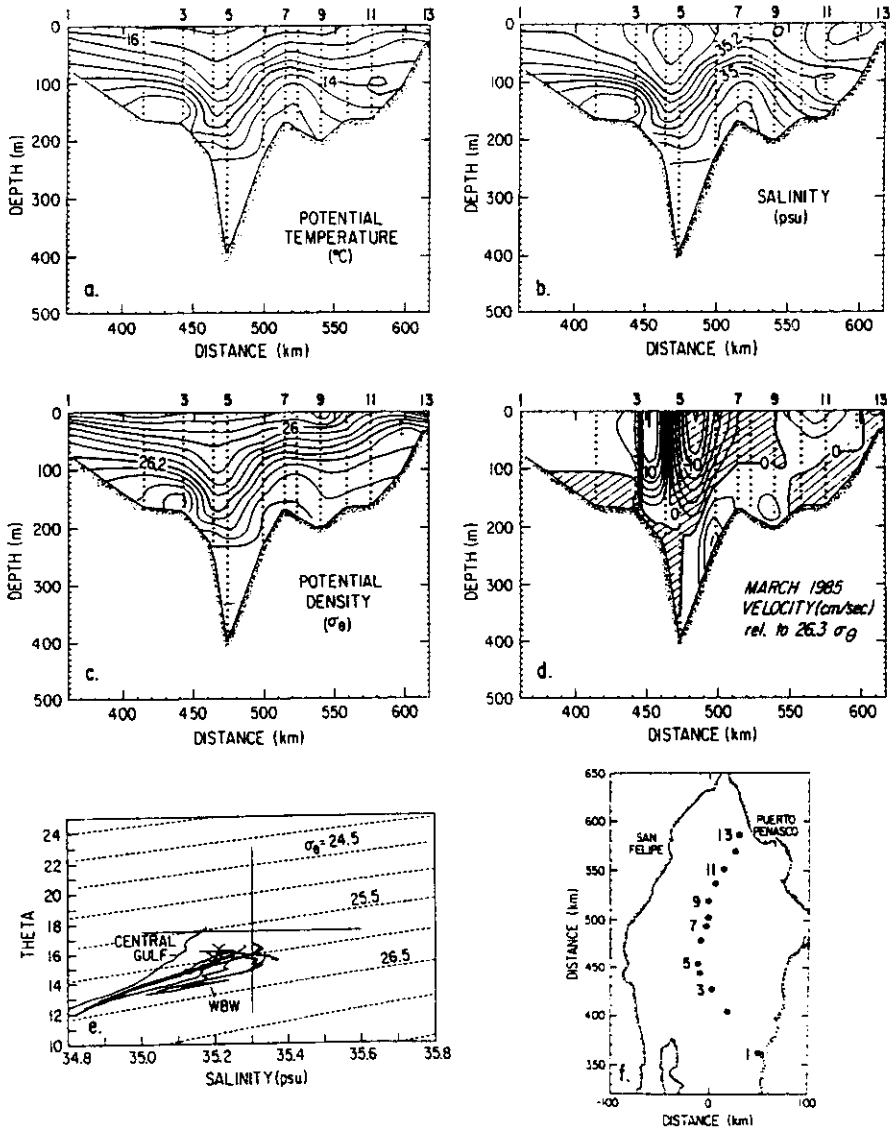

Fig. 16. Vertical section through the gyre center (March 1985): (*a*) temperature, (*b*) salinity, (*c*) density, (*d*) velocity relative to 26.3 σ_θ roughly 100 m depth, (*e*) temperature versus salinity, and (*f*) station locations. Note the depressed isopycnals in the center of the gyre and the elevated temperatures and salinities found at depth in the gyre.

26

GC25/26

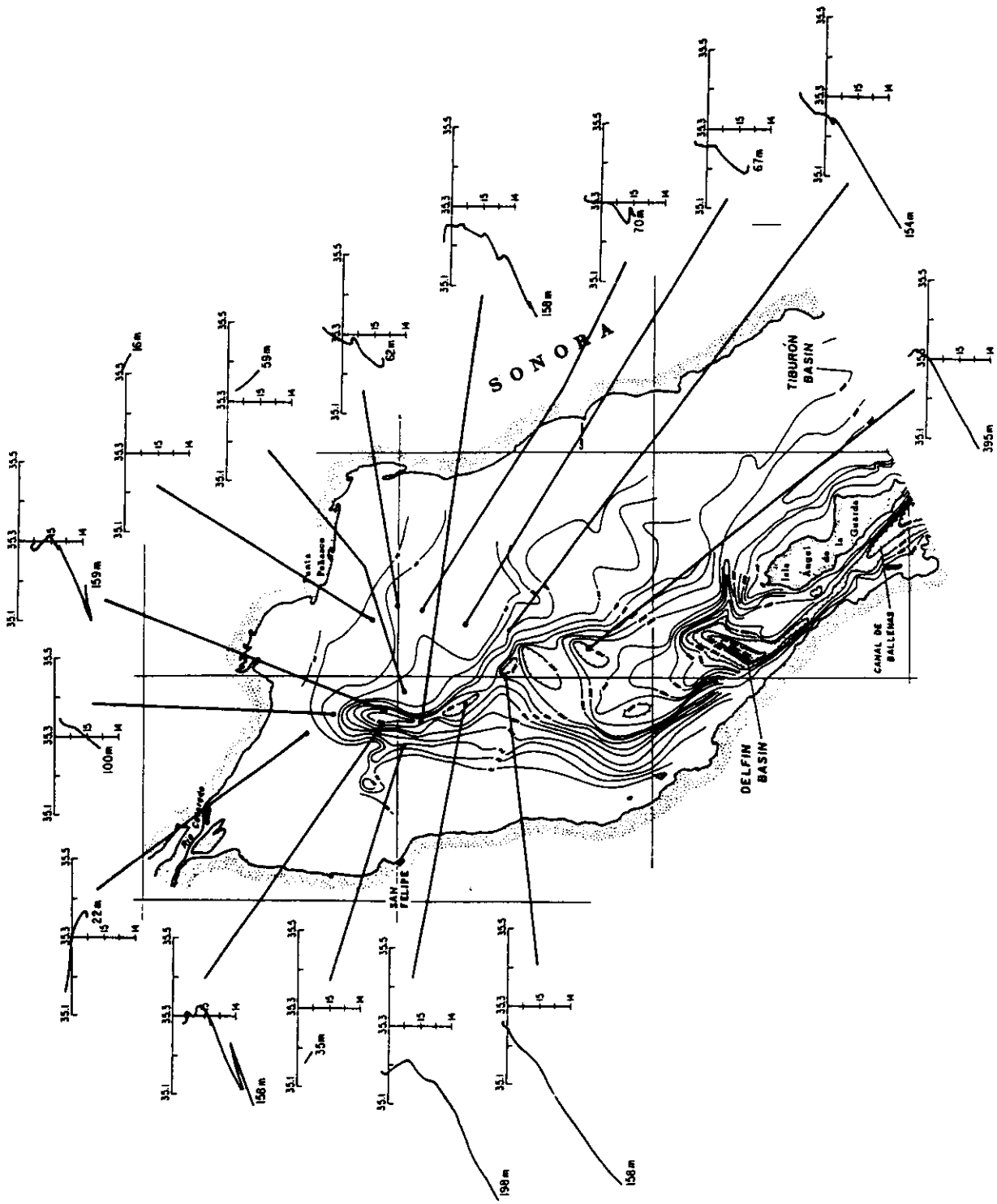

Fig. 9. March 1985: Horizontal distribution of T–S structure indicating local convection. Inset plots are T–S curves with the scale shown in the bottom right corner. Convection appears to be limited to the vicinity of the Wagner Basin.

GC 27

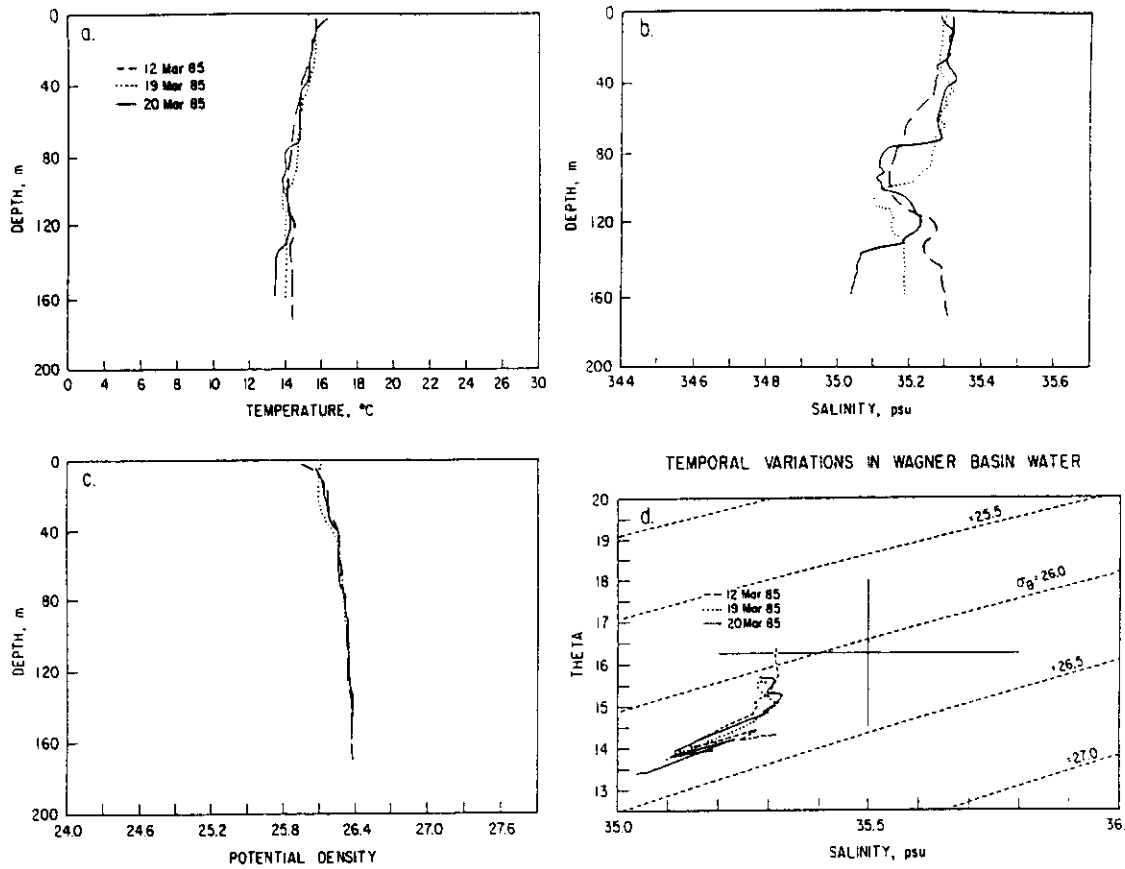

Fig. 8. Short term variability of water mass characteristics in the Wagner Basin during March 1985. Three stations were occupied at the same location in the center of the basin on the March 12, 19, and 20. These stations occurred 9 days after, during and 1 day after substantial storms, respectively, as can be seen in the wind records shown in Figure 10. Shown here are (*a*) temperature, (*b*) salinity, (*c*) density, and (*d*) potential temperature versus salinity for the three stations.

28

GC28